Synthesis, in Vitro Pharmacology, and Molecular Modeling of Very Potent Tacrine−Huperzine A Hybrids as Acetylcholinesterase Inhibitors of Potential Interest for the Treatment of Alzheimer's Disease

Pelayo Camps,*[,†] Rachid El Achab,[†] Diana Marina Görbig,[†] Jordi Morral,[†] Diego Muñoz-Torrero,[†] Albert Badia,[‡] Josep Eladi Baños,[‡] Nuria María Vivas,[‡] Xavier Barril,[§] Modesto Orozco,[▽] and Francisco Javier Luque[§]

Laboratori de Química Farmacèutica, Facultat de Farmàcia, Universitat de Barcelona, Av. Diagonal 643, E-08028 Barcelona, Spain, Departament de Farmacologia i de Terapèutica, Facultat de Medicina, Universitat Autònoma de Barcelona, 08193-Bellaterra, Barcelona, Spain, Departament de Físico-Química, Facultat de Farmàcia, Universitat de Barcelona, Av. Diagonal 643, E-08028 Barcelona, Spain, and Departament de Bioquímica, Facultat de Química, Universitat de Barcelona, Av. Martí i Franqués 1, E-08028 Barcelona, Spain

Received November 4, 1998

Eleven new 12-amino-6,7,10,11-tetrahydro-7,11-methanocycloocta[*b*]quinoline derivatives [tacrine (THA)−huperzine A hybrids, *rac*-**21**−**31**] have been synthesized as racemic mixtures and tested as acetylcholinesterase (AChE) inhibitors. For derivatives unsubstituted at the benzene ring, the highest activity was obtained for the 9-ethyl derivative *rac*-**20**, previously prepared by our group. More bulky substituents at position 9 led to less active compounds, although some of them [9-isopropyl (*rac*-**22**), 9-allyl (*rac*-**23**), and 9-phenyl (*rac*-**26**)] show activities similar to that of THA. Substitution at position 1 or 3 with methyl or fluorine atoms always led to more active compounds. Among them, the highest activity was observed for the 3-fluoro-9-methyl derivative *rac*-**28** [about 15-fold more active than THA and about 9-fold more active than (−)-huperzine A]. The activity of some THA−huperzine A hybrids (*rac*-**19**, *rac*-**20**, *rac*-**28**, and *rac*-**30**), which were separated into their enantiomers by chiral medium-pressure liquid chromatography (chiral MPLC), using microcrystalline cellulose triacetate as the chiral stationary phase, showed the eutomer to be always the levorotatory enantiomer, their activity being roughly double that of the corresponding racemic mixture, the distomer being much less active. Also, the activity of some of these compounds inhibiting butyrylcholinesterase (BChE) was tested. Most of them [*rac*-**27**−**31**, (−)-**28**, and (−)-**30**], which are more active than (−)-huperzine A as AChE inhibitors, turned out to be quite selective for AChE, although not so selective as (−)-huperzine A. Most of the tested compounds **19**−**31** proved to be much more active than THA in reversing the neuromuscular blockade induced by *d*-tubocurarine. Molecular modeling of the interaction of these compounds with AChE from *Torpedo californica* showed them to interact as truly THA−huperzine A hybrids: the 4-aminoquinoline subunit of (−)-**19** occupies the same position of the corresponding subunit in THA, while its bicyclo[3.3.1]nonadiene substructure roughly occupies the same position of the corresponding substructure in (−)-huperzine A, in agreement with the absolute configurations of (−)-**19** and (−)-huperzine A.

Introduction

It is well-known that many neurotransmitter systems are implicated in the etiology of Alzheimer's disease (AD), a cholinergic deficit having being clearly established.[1−5] Accordingly, enhancement of the central cholinergic function has been regarded as one of the most promising approaches for treating AD patients, mainly by means of acetylcholinesterase (AChE) inhibitors[6,7] such as the recently marketed tacrine (THA, Cognex, **1**),[8] donepezil (Aricept, **2**),[9] or rivastigmine (Exelon, **3**)[10] (Figure 1).

Much work has been done in the past few years for the development of more potent, selective, and safe AChE inhibitors.[11] Among them, huperzine A, an alkaloid isolated from *Huperzia serrata*, has been proposed as a potent drug for treating AD. Some huperzine A derivatives (**5** and **6**) more potent than the natural product were also developed by modeling the interaction of huperzine A[12] (**7**) with AChE.[13] Some time ago, we carried out the synthesis and evaluation of several THA-related AChE inhibitors such as **4**,[14] formally derived from THA by molecular duplication. Moreover, some new THA-based compounds, containing two THA subunits with their amino groups connected by an oligomethylene chain, such as **8**, were designed taking into account the existence of two binding sites for THA in AChE.[15] Recently, we have published the synthesis and pharmacological evaluation of several derivatives, designed by combination of the pharmacophores of huperzine A (carbobicyclic substructure) and THA (4-aminoquinoline substructure).[16] Although compound **9**, which incorporated the carbobicyclic substructure of huperzine A and the 4-aminoquinoline substructure of THA, was less active than THA, the derivatives *rac*-**19** and *rac*-**20** (Scheme 1), lacking the ethylidene substituent at the methylene bridge, were 2−4-fold more active than THA. It is worth noting that the introduction of

† Laboratori de Química Farmacèutica..
‡ Departament de Farmacologia i de Terapèutica.
§ Departament de Físico-Química.
▽ Departament de Bioquímica.

10.1021/jm980620z CCC: $18.00
Published on Web 07/30/1999

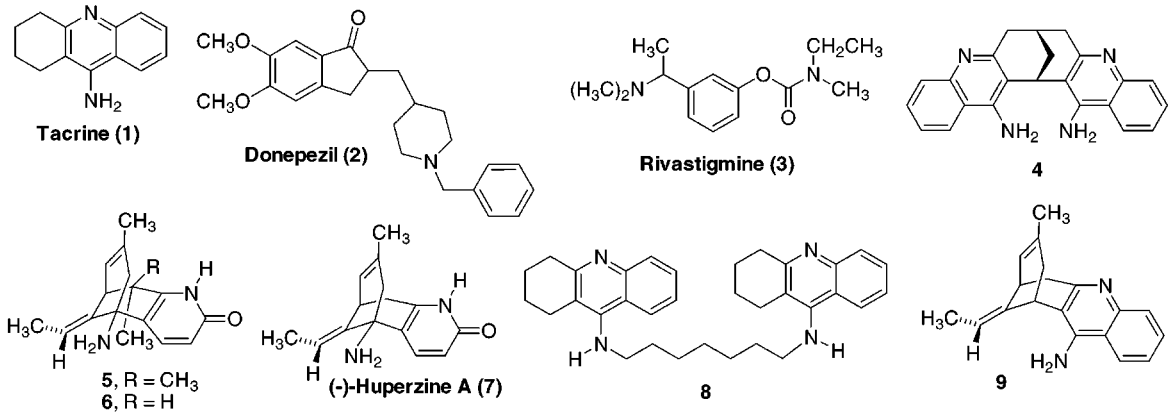

Figure 1. Structures of some known AChE inhibitors.

Scheme 1. Synthetic Procedure for the Preparation of Hybrids *rac*-**19**−**31**

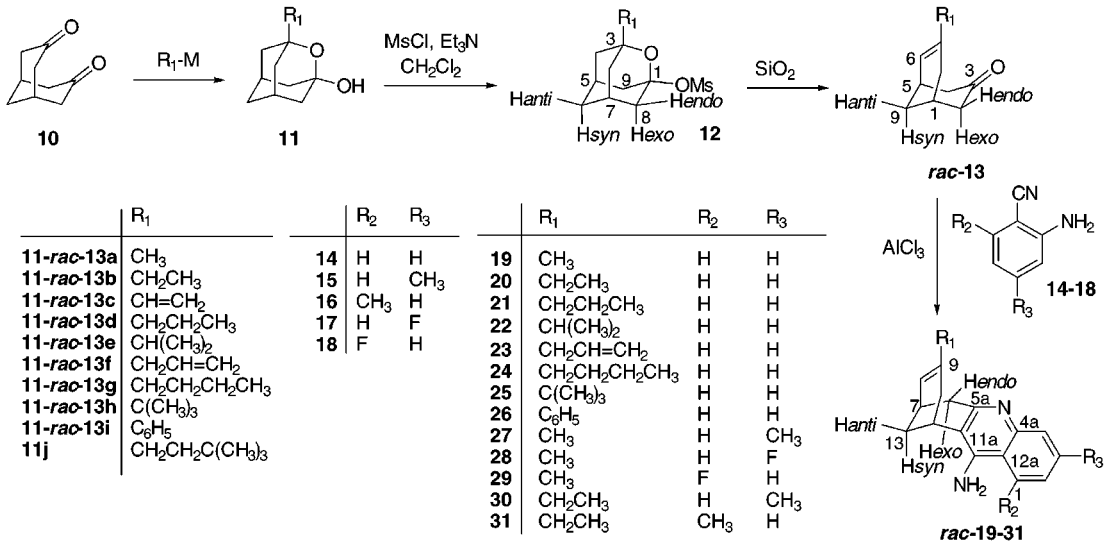

	R_1
11-*rac*-**13a**	CH_3
11-*rac*-**13b**	CH_2CH_3
11-*rac*-**13c**	$CH{=}CH_2$
11-*rac*-**13d**	$CH_2CH_2CH_3$
11-*rac*-**13e**	$CH(CH_3)_2$
11-*rac*-**13f**	$CH_2CH{=}CH_2$
11-*rac*-**13g**	$CH_2CH_2CH_2CH_3$
11-*rac*-**13h**	$C(CH_3)_3$
11-*rac*-**13i**	C_6H_5
11j	$CH_2CH_2C(CH_3)_3$

	R_2	R_3
14	H	H
15	H	CH_3
16	CH_3	H
17	H	F
18	F	H

	R_1	R_2	R_3
19	CH_3	H	H
20	CH_2CH_3	H	H
21	$CH_2CH_2CH_3$	H	H
22	$CH(CH_3)_2$	H	H
23	$CH_2CH{=}CH_2$	H	H
24	$CH_2CH_2CH_2CH_3$	H	H
25	$C(CH_3)_3$	H	H
26	C_6H_5	H	H
27	CH_3	H	CH_3
28	CH_3	H	F
29	CH_3	F	H
30	CH_2CH_3	H	CH_3
31	CH_2CH_3	CH_3	H

substituents such as alkyl, alkoxy, or oxo at the methylene bridge as well as the substitution of this bridge by an *o*-phenylene one or the substitution of the benzene ring of the 4-aminoquinoline moiety by a cyclopentene ring resulted in much less active compounds. These results led us to prepare new derivatives of **19** and **20**, bearing different alkyl groups at position 9 or substituted on the 4-aminoquinoline moiety, and to evaluate the pharmacological activity of both enantiomers of some of these compounds.[17] In addition, the modeling of the interaction of these hybrid compounds with the AChE of *Torpedo californica*[18] was also studied, taking advantage of the previous work carried out with THA[19] and (−)-huperzine A.[20]

Chemistry

The synthesis of compounds *rac*-**21**−**31** was carried out by Friedländer condensation of the corresponding enone *rac*-**13** and *o*-aminobenzonitrile **14**−**18** (Scheme 1).

Most of the required starting enones have been previously described: *rac*-**13a**,[21−23] *rac*-**13b**,**d**,**g**,**i**,[23] and *rac*-**13c**.[17] Enones *rac*-**13e**,**f** were prepared following a procedure previously developed by our group, based on the silica gel-promoted fragmentation of the mesylates **12** derived from the corresponding 3-alkyl-2-oxa-1-adamantanols **11**.[23] Oxaadamantanols **11**, conveniently substituted at position 3, were obtained by reaction of diketone **10** with the required organolithium or organomagnesium reagents. For a given oxaadamantanol, yields were better using the organolithium reagent.[23] In this way, using vinyllithium and allyllithium, oxaadamantanols **11c**,**f** were obtained in 59% and 57% yield, respectively. Reaction of **10** with isopropyllithium did not afford the desired oxaadamantanol **11e**, no defined product being isolated from this reaction. Also, treatment of **10** with *tert*-butyllithium did not afford the expected oxaadamantanol **11h**, 3-(3,3-dimethylbutyl)-2-oxa-1-adamantanol (**11j**) being isolated instead, in 45% yield. The formation of **11j** can be rationalized by reaction of **10** with 3,3-dimethylbutyllithium. This organolithium reagent can be formed by reaction of *tert*-butyllithium with ethylene,[24] formed by cleavage of the THF on reaction with *tert*-butyllithium.[25] These negative results can be explained taking into account that some carbonyl compounds, such as diketone **10**, are susceptible to undergo some so-called abnormal reactions (enolization, reduction, aldol condensation, or pinacol coupling) on attempted addition of simple organolithium or Grignard reagents. Organocerium reagents have been found to be extremely useful in these cases since these abnormal reactions are remarkably

suppressed.[26] Thus, organocerium reagents react readily with ketones at low temperature to give the addition products in good to high yields. In fact, reaction of diketone **10** with *i*-$PrCeCl_2$, prepared by treatment of *i*-PrLi with anhydrous $CeCl_3$,[27] afforded oxaadamantanol **11e** in 58% yield. Similarly, reaction of **10** with *t*-$BuCeCl_2$ gave **11h** in 54% yield. Although oxaadamantanols **11a**,**b** had been already prepared by reaction of diketone **10** with the corresponding organolithium compound (84% and 76% yield, respectively), we synthesized them more efficiently by using the corresponding organocerium reagent. Thus, treatment of commercial MeMgBr or EtMgBr with anhydrous $CeCl_3$, followed by addition of diketone **10**, led to oxaadamantanol **11a** or **11b** in higher yields (91% and 85%, respectively) than those previously obtained with the corresponding organolithium reagents.

Mesylates **12c**,**e**,**f**,**h** were prepared in high yields by reaction of the corresponding oxaadamantanols with methanesulfonyl chloride following a standard procedure.[28] Reaction of mesylates **12e**,**f** with silica gel in CH_2Cl_2 at room temperature for 3−4 h afforded the expected enones *rac*-**13e**,**f** in 43% and 50% yield, respectively, after column chromatography. In both cases, oxaadamantanols (**11e**,**f**) were also obtained as byproducts in 11% and 21% yield, respectively. The fragmentation of mesylate **12h** was even easier. In this case, a simple heating of a suspension of **12h** in hexane under reflux for 30 min afforded the expected enone *rac*-**13h** in 80% yield. However, enone **13c** could not be obtained from mesylate **12c** neither by reaction with silica gel nor with concentrated H_2SO_4 in methanol, complex mixtures of products being obtained instead.

Reaction of enones *rac*-**13d**,**g**,**i**, previously prepared in our group,[23] and of the new ones *rac*-**13e**,**f**,**h** with 2-aminobenzonitrile (**14**) catalyzed by $AlCl_3$ in 1,2-dichloroethane under reflux gave rise in moderate to excellent yields to the corresponding racemic aminoquinolines *rac*-**21**−**26**. These compounds were transformed into the corresponding hydrochlorides and crystallized from the appropriate solvent (see Experimental Section). Worthy of note, as previously observed,[16] only the shown aminoquinolines, having the heterocyclic ring and the endocyclic C−C double bond in an *anti*-arrangement, were observed. This fact may be explained taking into account the mechanism of this reaction, which is illustrated in Scheme 2 for the reaction of enone **13a** and *o*-aminobenzonitrile (**14**). Reaction of **13a** and **14** would give imine **32** which would be in equilibrium with two regioisomeric enamines (**33** and **34**), the *anti*-enamine **33** being reasonably the thermodynamically more stable, as is the case for the *anti*-enamine **37**, obtained by reaction of ketone **36** with pyrrolidine (Scheme 3).[29] Similarly, aminoquinoline **19** is expected to be more stable than **35**, and this greater stability must also be reflected in the transition states leading from enamines **33** and **34** to aminoquinolines **19** and **35**. If the above hypothesis is correct, kinetically controlled Friedländer cyclization of the *anti*-enamine **33** would give preferentially the *anti*-aminoquinoline **19**, the only observed regioisomer. In no case were the *syn*-aminoquinolines corresponding to **19**−**26** observed.

The best AChE inhibitory activities of compounds *rac*-**19**−**26** were observed for the methyl and ethyl derivatives *rac*-**19** and *rac*-**20** (see Pharmacology). These results prompted us to carry out the synthesis and evaluation of derivatives of **19** and **20**, bearing one alkyl or halogen substituent at different positions on the benzene ring. Thus, reaction of enones *rac*-**13a**,**b** with 2-amino-4-methylbenzonitrile (**15**) catalyzed by $AlCl_3$ in 1,2-dichloroethane under reflux afforded the corresponding racemic aminoquinolines *rac*-**27** and *rac*-**30**, in 91% and 25% yield, respectively.

However, the Friedländer condensation of *rac*-**13b** with 2-amino-6-methylbenzonitrile (**16**) in 1,2-dichloroethane under reflux for 7 h did not give the expected aminoquinoline *rac*-**31**, adamantanediamine **38** being isolated instead in low yield. When this reaction was carried out under more vigorous conditions (1,2-dibromoethane under reflux for 18 h), aminoquinoline *rac*-**31** was obtained in 65% yield. Steric hindrance during the carbon−carbon bond-forming step of the Friedländer reaction due to the 6-methyl substituent of **16** may explain the observed rate decrease for the formation of *rac*-**31**.

The formation of compound **38** can be rationalized, as shown in Scheme 4, under acid catalysis. Condensation of enone *rac*-**13b** with aminobenzonitrile **16** would give an imine. Acid-catalyzed isomerization of the endocyclic carbon−carbon double bond to an exocyclic position followed by electrophilic addition of the protonated imine would give a carbocation which, on reaction with a second molecule of **16**, would give **38**. This reaction sequence must not be much affected by the presence of the methyl group of **16**, and thus it can take

Scheme 2. Alternative Pathways in the Friedländer Reaction of Enones **13** and Aminobenzonitrile **14**

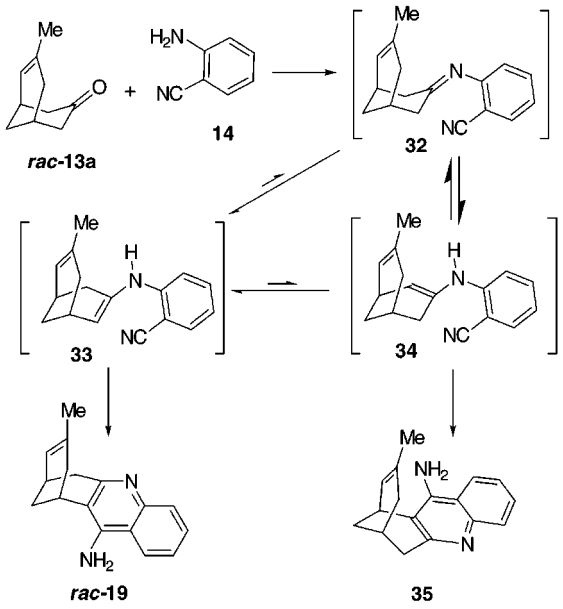

Scheme 3. Main Enamine **37** Formed from Keto Carbamate **36**

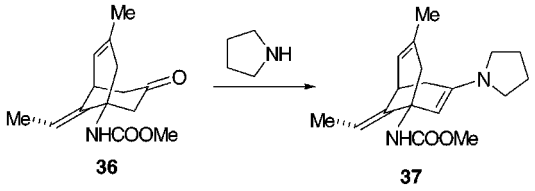

Scheme 4. Possible Mechanistic Pathway for the Formation of Adamantane Derivative **38** from Enone *rac*-**13b** and Aminobenzonitrile **16**

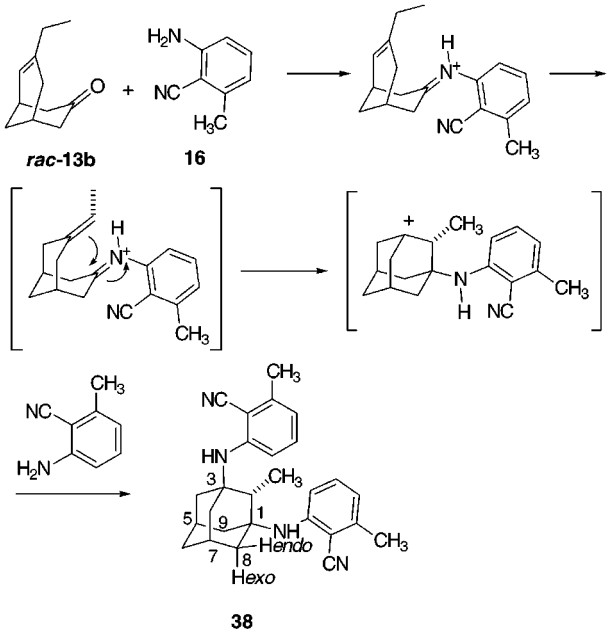

place under moderate reaction conditions, if an acid catalyst is present.

The Friedländer condensation of *rac*-**13a** with 2-amino-4-fluorobenzonitrile (**17**) and 2-amino-6-fluorobenzonitrile (**18**) under standard conditions allowed us to obtain the fluorinated derivatives *rac*-**28** and *rac*-**29** in 74% and 66% yield, respectively.

The excellent pharmacological results obtained with *rac*-**28** and *rac*-**30** (see Pharmacology) led us to carry out their chromatographic resolution by chiral MPLC in a manner similar to that described for *rac*-**19** and *rac*-**20**.[17] In this way we could obtain both enantiomers of compounds **28** and **30** in an adequate scale for the pharmacological tests. The (7*R*,11*R*)-configuration was assigned to (+)-**28** and (+)-**30** and the (7*S*,11*S*)-configuration to (−)-**28** and (−)-**30**, taking into account the configuration of the (+)- and (−)-enantiomers of a closely related derivative, which was determined by X-ray diffraction analysis.[17]

All of the new compounds have been fully characterized through their spectroscopic and analytical data (IR, ^{1}H and ^{13}C NMR spectra, and elemental analysis). The ^{1}H and ^{13}C NMR spectra of all of these compounds were fully assigned through the COSY ^{1}H/^{1}H and COSY ^{1}H/^{13}C spectra. Differentiation among the pairs of protons 8(9)-H*endo*/*exo* and 4(10)-H*endo*/*exo* of mesylates **12** could be easily carried out taking into account the presence in the COSY ^{1}H/^{1}H spectra of cross-peaks corresponding to *W*-couplings between the *exo* protons of these positions. The more deshielded proton of the 8(9)-H*endo*/*exo* pair was assigned to the *endo* one. In our previous work,[23] the assignment of the pair of protons 8(9)-H*endo*/*exo* of some related mesylates carried out by comparison with the corresponding alcohols was interchanged, since no *W*-coupling between the *exo* protons of these positions was observed. For the assignment of the quaternary carbon atoms of compounds *rac*-**21**−**31**, previous work[14,16] was taken into account.

Table 1. Pharmacological Data of Tacrine, (−)-Huperzine A, and Compounds **19**−**31**·HCl[a]

compd	IC$_{50}$ (nM)[a] AChE	IC$_{50}$ (nM)[a] BChE	BChE IC$_{50}$/ AChE IC$_{50}$	AI$_{50}$ (nM)
tacrine	130 ± 10	43.9 ± 1.7	0.34	71700
(−)-huperzine A	74 ± 5.5	>10^5	>10^3	*b*
rac-**19**	65 ± 15	126 ± 21	1.9	176
(+)-**19** (87% ee)	329 ± 58	316 ± 12	0.96	*c*
(−)-**19** (90% ee)	47.1 ± 6.3	89.0 ± 0.2	1.9	613
rac-**20**	38.5 ± 4	79.3 ± 9.7	2.1	84
(+)-**20** (99% ee)	888 ± 141	109 ± 7	0.12	*d*
(−)-**20** (99% ee)	27.4 ± 3.1	63.3 ± 8.6	2.3	336
rac-**21**	431 ± 94	*b*		260
rac-**22**	103 ± 17	*b*		*b*
rac-**23**	150 ± 16	*b*		*d*
rac-**24**	280 ± 87	*b*		*d*
rac-**25**	267 ± 87	*b*		*b*
rac-**26**	126 ± 8	*b*		*d*
rac-**27**	12.4 ± 2.3	449 ± 40	36	*b*
rac-**28**	8.5 ± 1.8	197 ± 30	23	8.0
(+)-**28** (99% ee)	1480 ± 180	2930 ± 20	2	*b*
(−)-**28** (99% ee)	3.49 ± 0.84	138 ± 20	40	48.6
rac-**29**	31.4 ± 0.8	543 ± 89	17	73.5
rac-**30**	12.0 ± 2.2	208 ± 27	17	*b*
(+)-**30** (96% ee)	485 ± 57	115 ± 17	0.24	*d*
(−)-**30** (97% ee)	4.5 ± 0.8	347 ± 39	77	213
rac-**31**	29.8 ± 6.2	512 ± 90	17	566

[a] Values are expressed as mean ± standard error of the mean of at least four experiments. IC$_{50}$, 50% inhibitory concentration of acetylcholinesterase (from bovine erythrocytes) or butyrylcholinesterase (from human serum) activity; AI$_{50}$, drug concentration that reaches 50% of antagonism index (AI). All compounds were used in the form of hydrochlorides, and the values were determined taking into account the water of crystallization deduced from the elemental analysis. [b] Not determined. [c] Only 22.8% reversion was obtained at 10 μM. [d] No reversion at 10 μM concentration.

Pharmacology

To determine the potential interest of compounds **19**−**31** for the treatment of AD, their AChE inhibitory activity was assayed by the method of Ellman et al.[30] on AChE from bovine erythrocytes. For the most active compounds and to establish their selectivity, their butyrylcholinesterase (BChE) inhibitory activity was also assayed by the same method on human serum BChE. Most of them were further analyzed in a peripheral cholinergic synapse, such as skeletal neuromuscular junction. In this analysis, the ability to reverse the *d*-tubocurarine-induced neuromuscular blockade, a well-known effect of AChE inhibitors,[31] was tested.

Table 1 summarizes the data comparing AChE and BChE inhibition as well as the ratio between BChE and AChE activities and the reversion of the neuromuscular blockade of the hybrid compounds and the reference compounds THA and (−)-huperzine A. As this table shows, (−)-huperzine A is about 2-fold more active than tacrine, while hybrid compounds *rac*-**20** and *rac*-**27**−**31** are clearly more active than (−)-huperzine A as AChE inhibitors. It is worth noting that the enantioenriched compounds (−)-**19**, (−)-**20**, (−)-**28**, and (−)-**30** are about 2-fold more active than their racemic mixtures, while their enantiomers are by far less potent. The rest of the compounds (*rac*-**21**−**26**) are slightly less potent than (−)-huperzine A.

About the BChE activity, it is worth noting that THA is 3-fold more active toward BChE than toward AChE, while (−)-huperzine A is highly selective for AChE. Among the hybrid compounds, the more active derivatives [*rac*-**27**−**31**, (−)-**28**, and (−)-**30**] are quite selective inhibiting AChE. Most of these compounds are also

clearly more potent than THA in reversing the neuromuscular blockade, while others show lower or no activity when used at a concentration of 10 μM.

Discussion

Recently we reported that *rac*-**19** and *rac*-**20** were about 2- and 4-fold more active than THA as AChE inhibitors. An examination of the results in Table 1 shows that the substitution of the methyl or ethyl group at position 9 (R_1 substituent), present in **19** and **20**, by different alkyl (propyl, isopropyl, butyl, *tert*-butyl), phenyl, or allyl substituents leads to compounds which are equipotent to or somewhat less active than THA. Thus, the 9-isopropyl-, 9-allyl-, and 9-phenyl-substituted aminoquinolines *rac*-**22**, *rac*-**23**, and *rac*-**26**, respectively, exhibited approximately the same AChE inhibitory activity than THA, while the introduction of a propyl (*rac*-**21**), butyl (*rac*-**24**), or *tert*-butyl (*rac*-**25**) group at position 9 results in an activity 2−3-fold lower.

On the other hand, the introduction of a methyl or fluorine substituent at positions 1 or 3 (R_2 and R_3 substituents) results in an enhanced AChE inhibitory activity, especially when this substituent is located at position 3. Thus, the 3-methyl derivatives *rac*-**27** and *rac*-**30** and the 3-fluoro derivative *rac*-**28** are 6-, 6-, and 9-fold more potent than (−)-huperzine A, respectively, while the 1-methyl and 1-fluoro derivatives *rac*-**31** and *rac*-**29** are approximately 2.5-fold more potent than (−)-huperzine A. The increase in the AChE activity of the 1- or 3-substituted derivatives *rac*-**27**−**31** parallels the results reported by Kawakami et al.[32] for other THA derivatives.

We have evaluated both enantiomers of some of these compounds (**19**, **20**, **28**, and **30**). Always the (−)-enantiomer is the more active one (eutomer). Taking into account their enantiomeric excesses (ee's), their activity is roughly 2-fold that of the corresponding racemic mixtures. Moreover, the (+)-enantiomers (distomers) are much less active than the corresponding racemic mixtures, especially if their activity is corrected for the presence of the (−)-enantiomer by assuming additive effects.

In connection with the AChE inhibitory activity of compounds **19**−**31**, some qualitative structure−activity relationships can be derived from the above data: (a) the optimal activity is found when there is a methyl or ethyl group at position 9 (bicyclo[3.3.1]nonadiene substructure); (b) the introduction of a methyl group or a fluorine atom at position 1 or 3 (aminoquinoline substructure) results in a highly enhanced activity, the 3-substituted derivatives being the more active compounds; (c) the levorotatory enantiomer of each racemic mixture is the more potent one.

Although it has not been completely clarified if the selectivity in inhibiting AChE versus BChE results in low peripheral cholinergic effects in AD patients,[33] we determined the BChE inhibitory activity of the more active compounds toward AChE (Table 1). Most of the compounds tested were very selective for AChE, especially *rac*-**27**−**31** (by factors between 17 and 36) and the levorotatory enantiomers of some of them [(−)-**28** and (−)-**30**, by factors of 40 and 77, respectively, the last one being the most selective]. Other compounds showed selectivity for the BChE such as (+)-**20** and (+)-**30**. Finally, (+)-**19** did not distinguish between both enzymes. Worthy of note, (−)-huperzine A is highly selective for AChE (see Table 1).

For the reversion of the neuromuscular blockade, the more active compounds are the fluorinated derivatives *rac*-**28**, (−)-**28**, and *rac*-**29** and also *rac*-**20** (8960-, 1475-, 975-, and 855-fold more potent than THA, respectively). Other compounds that are more potent than THA as AChE inhibitors, such as (−)-**19**, (−)-**20**, (−)-**30**, and *rac*-**31**, are also more active in this assay (120−340-fold more potent than THA). Compound *rac*-**21** exhibit greater activity than THA in this assay (275-fold) despite its lower AChE inhibitory activity. The discrepancy observed on the potency of racemates and enantiomers to inhibit AChE and to reverse neuromuscular blockade deserves further comment. The biochemical studies used (i.e., determination of AChE inhibition) test the ability of a compound to inhibit enzyme activity; therefore, they only analyze the drug effects in a single mechanism. The pharmacological testing (i.e., determination of neuromuscular blockade reversion) analyzes the magnitude of an effect regardless of the implicated mechanisms. The pharmacological testing adds valuable information over the biochemical studies, as it evaluates how the drug enhances the activity of a cholinergic synapse and not merely the action on an isolated enzyme. However, drugs may act in several targets (enzymes, receptors) at skeletal neuromuscular junctions,[34] and indeed, some actions, such as blockade of nerve potassium chanels or activation of presynaptic M_1 receptors, may facilitate neurotransmission at this level.[35] Thus, THA may enhance acetylcholine release besides its AChE inhibitory action.[36] We did not test each of these possibilities to explain the discrepancies between the effects of racemates and enantiomers. However, some preliminary and unpublished data have shown that some of the present compounds bind to M_1 receptors. Further work is in progress to gain more knowledge about these unexpected actions.

Molecular Modeling. To understand the recognition of **19** and to enable rational design of new derivatives, we examined different binding modes of **19** in AChE. Since **19** was conceived as a hybrid between THA and huperzine A, our working hypothesis was to assume that its binding to AChE shares some or all of the features that modulate the binding of THA and huperzine A. Accordingly, modeling of the interaction of **19** with the enzyme was based on the crystallographic structures of the AChE complexes with THA[19] and (−)-huperzine A.[20] To examine the suitability of the computational approach (see Molecular Modeling: Methods), calculations were extended to the binding of THA and the two enantiomers of huperzine A.

The energy-minimized structures of AChE complexed with THA and (−)-huperzine A reproduce the basic interactions between inhibitor and enzyme found in the crystallographic structures.[19,20] In the former complex (Figure 2, left), THA is stacked between Trp84 and Phe330 (the distance from THA to both indole and benzene rings varies from 3.5 to 3.9 Å). The $^+$NH group is hydrogen-bonded to the carbonyl oxygen of His440 (2.9 Å), and the exocyclic amino group is well-hydrated, three water molecules being less than 3.3 Å from the nitrogen atom. These water molecules play a relevant

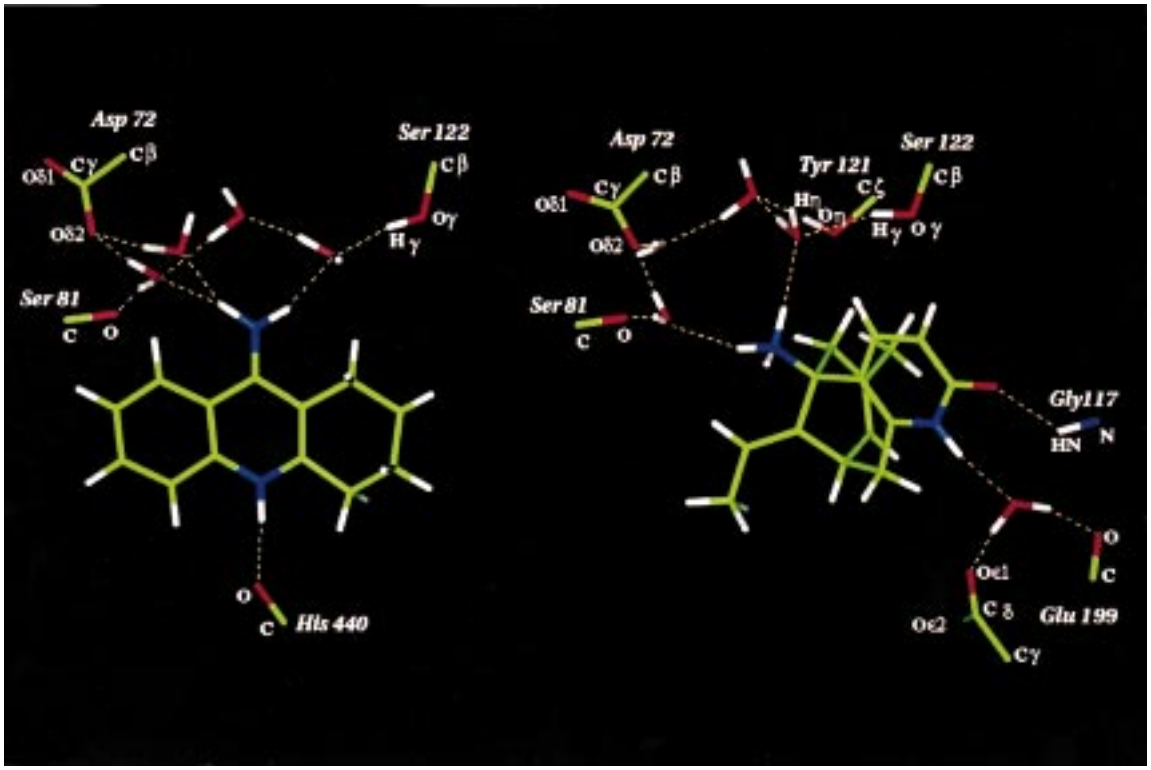

Figure 2. Plot of the main interactions between the protein and the ligand [left, tacrine; right, (−)-huperzine A]. Residues Trp84 and Phe330, which lie above and below the ligand in the picture, are not shown for the sake of clarity.

Table 2. Contributions (kcal/mol) of the Electrostatic, Lennard−Jones, and Solvent-Accessible Surface Terms to the Binding Free Energy Determined for THA and Enantiomers of Huperzine A

compd	ΔG_{ele}[a]	ΔE_{L-J}	ΔG_{SAS}
tacrine	−5.0 ± 2.1	−39.1	−4.0
(−)-huperzine A	−10.1 ± 2.1	−43.8	−4.3
(+)-huperzine A	−7.7 ± 1.6	−40.1	−4.5

[a] Average value of seven separate Poisson−Boltzmann calculations (see Molecular Modeling: Methods). The standard deviation is also given.

structural role, since they connect the NH_2 group to Ser122 and Asp72. In the AChE−(−)-huperzine A complex (Figure 2, right), the amido NH group is hydrogen-bonded to a water molecule (2.9 Å), which in turn interacts with Glu199, and to the main chain NH group of Gly117. The protonated amino group is surrounded by two water molecules lying approximately at 3.0 Å, which are hydrogen-bonded to other residues, like Asp72, Ser81, and Ser 122, or to other water molecules. Likewise, this ammonium group is around 4.8 Å from the five-membered ring of Trp84 and the benzene ring of Phe330. Finally, the carbonyl oxygen of His440 is close (around 3.1 Å) to the ethylidene methyl group, and the methyl group of the alicyclic bridge is about 4.3 Å from Phe290.

The results in Table 2 indicate that (−)-huperzine A binds better than THA.[37] Owing to the approximations underlying the computational model and to the fact that the inhibitory potency was determined from pharmacological assays performed in biological systems other than the *T. californica* enzyme, comparison with experimental data should be performed with caution. Nevertheless, the results in Table 2 show qualitative agreement with the experimental inhibitory data, which indicate that (−)-huperzine A (IC_{50} 47 nM inhibiting AChE from rat hippocampal crude homogenates[38] and IC_{50} 74 ± 5.5 nM inhibiting AChE from bovine erythrocytes obtained in this work) is somewhat more active than THA (IC_{50} 59 nM inhibiting AChE from rat brain[39] and IC_{50} 130 ± 10 nM inhibiting AChE from bovine erythrocytes obtained in this work).

To further analyze the reliability of calculations, we examined the interaction of (+)-huperzine A with AChE. The structure of (+)-huperzine A was oriented superimposing the pyridone ring with that of (−)-huperzine A in the crystallographic complex to keep all of the basic interactions of the NH, CO, and NH_3^+ groups. These interactions are retained in the energy-minimized structure, and the most notable difference with regard to the AChE−(−)-huperzine A complex is that the distance from the NH_3^+ group to Trp84 increases by ca. 1.4 Å. The results (Table 2) agree with the experimental fact that (+)-huperzine A inhibits the enzyme near 40-fold less potently than (−)-huperzine A.[40,41] The smaller binding of the (+)-enantiomer likely stems from the weakening of the interaction between the NH_3^+ group and Trp84, which supports the role of cation−π interactions in the binding of huperzine A,[13,20,42,43] in agreement with recent theoretical studies.[44,45]

Different binding modes that mimic the basic features of the interaction of either THA or (−)-huperzine A were examined for (−)-**19** (Figure 3). In mode 1, the quinoline rings of (−)-**19** and THA are matched, and the bicyclo[3.3.1]nonadiene substructure of (−)-**19** is over the alicyclic ring of THA. In mode 2, (−)-**19** has been rotated 180° along the largest molecular axis, so that the ^+NH and NH_2 groups are interchanged with regard to mode 1. Likewise, the molecule can be placed by rotating around the axis passing through the nitrogen atoms,

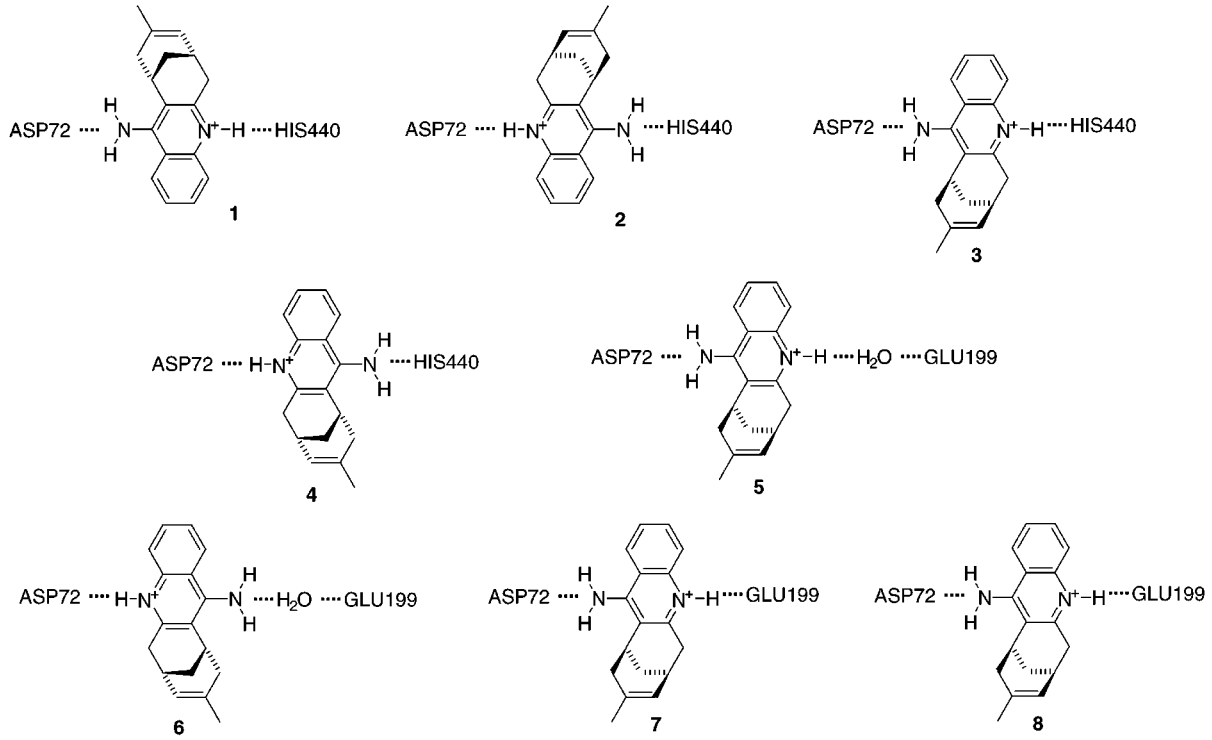

Figure 3. Schematic views of the different tacrine-like (1−4) and (−)-huperzine A-like (5−8) binding modes considered for compound (−)-**19**.

so that the bicyclo[3.3.1]nonadiene substructure is over the aromatic ring of THA (modes 3 and 4). With regard to the huperzine A-like binding motifs, (−)-**19** was oriented to mimic the water-mediated contact between the pyridone NH group of (−)-huperzine A and Glu199. This was accomplished connecting either the $^{+}$NH (mode 5) or NH_2 (mode 6) groups. In the two cases the bicyclo-[3.3.1]nonadiene substructure of (−)-**19** occupies the position of the corresponding substructure of (−)-huperzine A. Rotation of (−)-**19** around the axis passing through the nitrogen atoms, as was performed in the tacrine-like binding modes, was not considered, since these orientations are sterically hindered owing to unfavorable contacts with the AChE gorge. Finally, a direct interaction between the $^{+}$NH or NH_2 groups and Glu199 was also considered (modes 7 and 8). The same binding modes were considered for the (+)-enantiomer of **19**. In the energy-minimized structures there were no relevant changes in the position of the inhibitor with regard to the starting orientation, and the interactions were well-preserved. Likewise, the backbone in the AChE gorge showed slight changes, and no remarkable structural alterations were observed.

To discern the feasibility of the different binding modes, the computed binding free energies were compared in light of the inhibitory data, which indicate that the (−)-enantiomer is more effective in inhibiting the enzyme than the (+)-enantiomer (Table 1). Therefore, the putative binding mode should be that leading to a significant interaction energy and to a clear difference in the binding for related compounds, particularly (+)- and (−)-enantiomers. It is worth noting that comparison of the results for the two enantiomers benefits from cancellation of errors in the computed binding free energies. The results in Table 3 allow us to exclude the THA-like binding modes 2 and 4 and all of the huperzine A-like binding modes, which in some cases (modes 5 and 7) lead to better interaction of the (+)-enantiomer. In contrast, modes 1 and 3 provide the largest binding free energy differences and clearly distinguish the binding of the two enantiomers. Most of the interactions are similar in modes 1 and 3 (see Figure 4). The hybrid compound (−)-**19** is stacked between Trp84 and Phe330 (the indole and benzene rings are about 3.5−3.9 Å from the molecular plane). The $^{+}$NH group is hydrogen-bonded to the carbonyl oxygen of His440 (at around 2.9

Table 3. Contributions (kcal/mol) of the Electrostatic, Lennard−Jones, and Solvent-Accessible Surface Terms to the Binding Free Energy Determined for Compounds (+)- and (−)-**19** in Their Protonated Forms[a]

mode	ΔG_{ele}	ΔE_{L-J}	ΔG_{SAS}	$\Delta\Delta G$
		(−)-**19**		
1[b]	0.0	0.0	0.0	0.0
2	4.4	2.2	−0.2	6.4
3	−1.4	0.3	0.1	−1.2
4	4.3	2.1	−0.1	6.3
5	3.6	1.0	−0.1	4.5
6	2.1	−0.1	−0.1	1.9
7	4.3	2.8	−0.1	7.0
8	2.6	1.2	0.0	3.8
		(+)-**19**		
1	1.6	4.8	−0.1	6.3
2	4.8	1.9	−0.1	6.6
3	0.0	4.1	0.0	4.1
4	3.0	4.5	−0.2	7.3
5	3.5	−0.4	0.1	3.2
6	3.6	1.8	−0.2	5.2
7	1.9	2.6	0.0	4.5
8	1.7	4.2	0.0	5.9

[a] Values are relative to the results determined for the binding mode 1 of (−)-**19**. See Figure 3 for the schematic representation of the different binding modes. [b] The absolute values (kcal/mol) for the interaction of (−)-**19** in mode 1 are −7.7 ± 1.6, −44.9, and −4.5 for the electrostatic, Lennard−Jones, and solvent-accessible surface contributions.

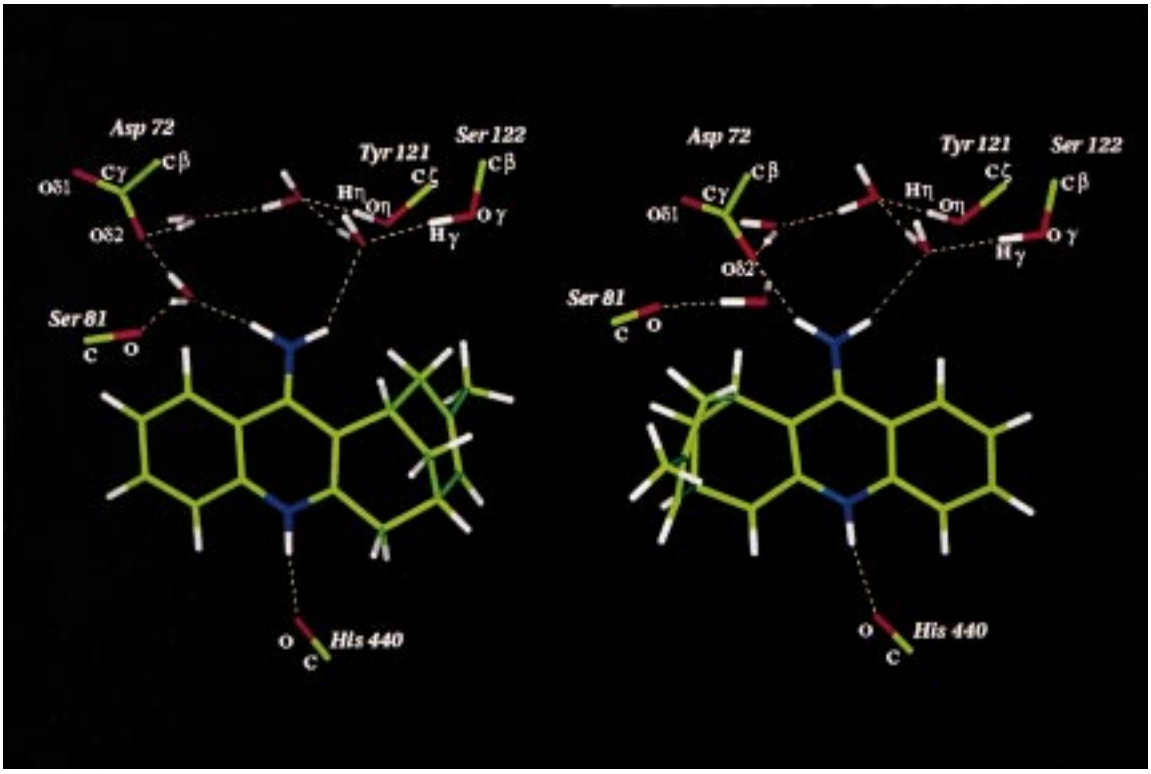

Figure 4. Plot of the main interactions between the protein and (−)-**19** for binding modes 1 (left) and 3 (right). Residues Trp84 and Phe330, which lie above and below the molecular plane of (−)-**19** in the figure, are not shown for the sake of clarity.

Table 4. Contributions (kcal/mol) of the Electrostatic, Lennard−Jones, and Solvent-Accessible Surface Terms to the Binding Free Energy Determined for (−)-**19** and Its 9-Ethyl [(−)-**20**], 9-Propyl [(−)-**21**], and 9-Methyl-3-fluoro [(−)-**28**] Derivatives in Their Protonated Forms, in Binding Modes 1 and 3[a]

compd	ΔG_{ele}	ΔE_{L-J}	ΔG_{SAS}	$\Delta\Delta G$
		Mode 1		
(−)-**19**	0.0	0.0	0.0	0.0
(−)-**20**	−0.1	−0.3	−0.3	−0.7
(−)-**21**	1.8	−0.4	−0.4	1.0
(−)-**28**	−0.4	−1.0	0.0	−1.4
		Mode 3		
(−)-**19**	0.0	0.0	0.0	0.0
(−)-**20**	3.9	−1.0	−0.1	2.8
(−)-**21**	5.2	−0.7	−0.4	4.1
(−)-**28**	3.3	−0.2	0.0	3.1

[a] Values are relative to the results determined for binding modes 1 and 3 of (−)-**19** (see Table 3).

Å). The exocyclic amino group is well-hydrated, and the water molecules connect (−)-**19** to the residues Asp72, Ser81, Tyr121, and Ser122. Regarding the bicyclo[3.3.1]-nonadiene substructure of (−)-**19**, the methyl group at position 9 lies in a pocket formed by the residues Phe290, Phe330, and Phe331 in mode 1, whereas it occupies a region surrounded by Trp84, Trp432, and Met83 in mode 3.

The suitability of modes 1 and 3 was further examined from calculations performed for the derivatives 9-ethyl [(−)-**20**], 9-propyl [(−)-**21**], and 9-methyl-3-fluoro [(−)-**28**], whose inhibitory activity exhibits clear trends compared to that of (−)-**19** (see Table 1). These trends are reflected in the results given in Table 4, since extension from 9-ethyl to 9-propyl makes the binding less favored, and the binding of the 9-methyl-3-fluoro derivative is comparable or slightly better than that of the 9-ethyl derivative. However, in mode 3 compounds (−)-**20** and (−)-**28** interact worse than (−)-**19** by nearly 3 kcal/mol, which disagrees with the measured change in their inhibitory activity relative to the parent 9-methyl compound (see Table 1). On the contrary, the binding of (−)-**20** and (−)-**28** is slightly better than that of (−)-**19** when mode 1 is considered, in agreement with the experimental inhibitory data.

The preceding discussion suggests us to propose mode 1 as a putative binding model for the hybrid compounds. As a final test, we performed a 500-ps molecular dynamics simulation (see Molecular Modeling: Methods) of the AChE−(−)-**19** complex with the inhibitor oriented following binding mode 1. The structural analysis showed that the complex remains stable along all the simulations without suffering remarkable changes in the interactions with the enzyme residues contributing to the binding. In addition, since human AChE contains a Tyr residue instead of Phe330, we examined the effect of this substitution on the binding of **19** by replacing Phe330 by Tyr in the last structure collected in the molecular dynamics simulation. The complex between (−)-**19** and the Phe330→Tyr enzyme remained stable during a subsequent 500-ps molecular dynamics simulation. After energy minimization of the last structure collected in this latter simulation, the computed binding free energy of (−)-**19** was found to be 7.2 kcal/mol better than that of the (+)-enantiomer, a value close to that reported in Table 3 (6.3 kcal/mol) for the *T. californica* enzyme. Therefore, the Phe330→Tyr substitution has no marked influence on the interactions mentioned above for binding mode 1.

It is worth emphasizing that mode 1 mixes effectively some of the binding features of THA and (−)-huperzine A. Thus, the NH_2 groups of THA and (−)-**19** and the

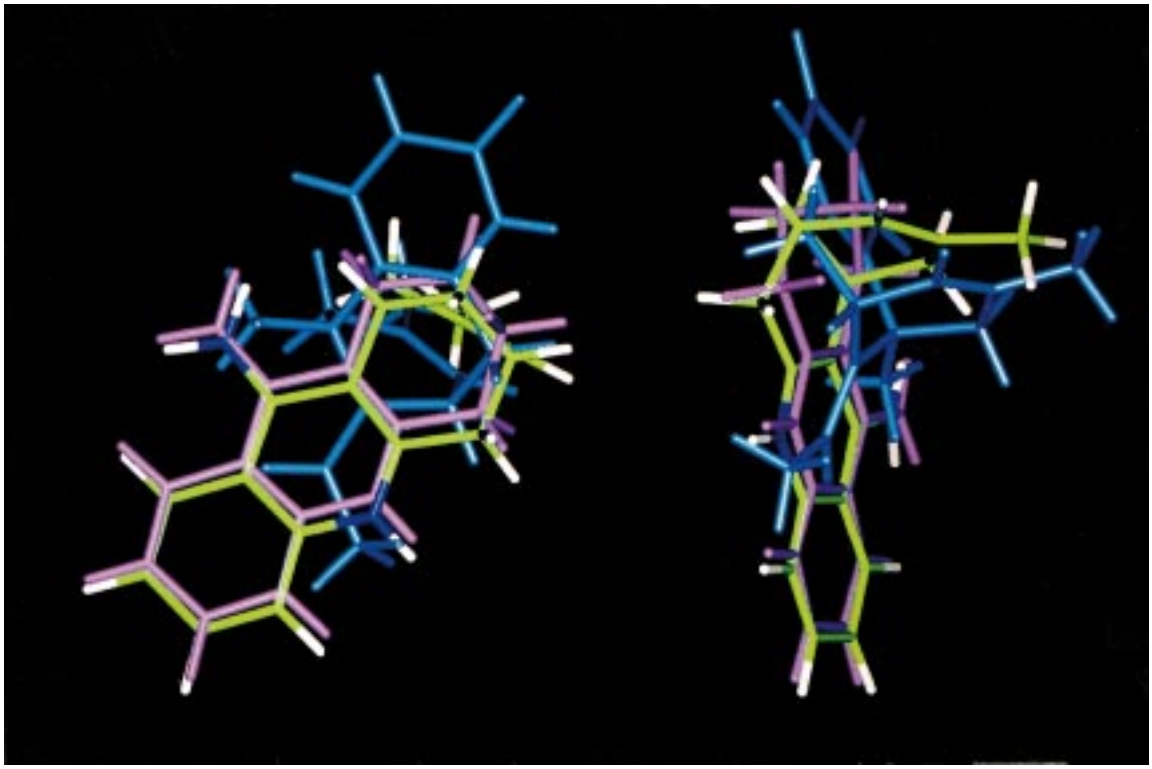

Figure 5. Two views of the superimposition of the inhibitors tacrine (magenta), (−)-huperzine A (blue), and (−)-**19** (green) in the orientations corresponding to their energy-minimized structures of the inhibitor−AChE complexes.

NH_3^+ group of (−)-huperzine A occupy nearly the same positions in the binding pocket (see Figure 5, left), which allows to share a common set of interactions in this region. Indeed, the quinoline ring of (−)-**19** fits the corresponding substructure in THA (Figure 5, left). Therefore, attachment of substituents to the aromatic ring in either (−)-**19** or THA should have an analogous effect on the inhibitory activity. This is confirmed by the available experimental data, which indicate that attachment of a fluorine atom at position 6 of THA increases the activity by a factor of 2.5,[32] and the same substitution in *rac*-**19** gives *rac*-**28**, which is 7.6-fold more active than *rac*-**19**. The same effect is observed when a chlorine atom is attached to the same position in THA and 1,4-methylenetacrine[46] and in dihydroquinazoline-based AChE inhibitors.[47] On the other hand, the bicyclo[3.3.1]nonadiene subunit of (−)-**19** lies in the same position occupied by the corresponding fragment of (−)-huperzine A within the AChE binding site (Figure 5, right), in accordance with their absolute configurations.[17] Again, the introduction of substituents in this subunit should lead to parallel changes in the inhibitory activity for the two compounds. To the best of our knowledge, the inhibitory potency of (−)-huperzine A derivatives with the methyl group at position 7 replaced by hydrogen, ethyl, propyl, or butyl groups has not been reported yet. Nevertheless, replacement of methyl by phenyl decreases the inhibitory activity by at least 1000-fold.[48] The same effect, although much less pronounced, occurs in *rac*-**19** upon substitution of the 9-methyl group by larger substituents such as propyl, butyl, isopropyl, *tert*-butyl, and phenyl (Table 1). Finally, let us note that these analogies concerning the effect of substituents cannot be realized if one assumes that the hybrid compound binds according to binding mode 3.

Even though the involvement of other binding sites cannot be ruled out,[49] the preceding considerations suggest that mode 1 can be considered to be a putative binding model to rationalize the AChE inhibitory activity of the hybrid derivatives. On the basis of the present results, future studies directed at developing hybrid compounds with improved inhibitory potency will be valuable to gain better understanding on the structural requirements involved in binding.

Conclusion

The AChE inhibitory activity of the THA−huperzine A hybrids *rac*-**19**−**31** herein described shows that, for better activity, the substituent R_1 at position 9 must be ethyl or methyl. More bulky substituents and also the absence of substituents at this position[16] lead to less active compounds. Substitution at position 1 (R_2) or 3 (R_3) with a methyl or fluorine atom always leads to increased AChE inhibitory activity. For a given substituent, the activity is higher when the substituent is located at position 3 (IC_{50} *rac*-**31**/IC_{50} *rac*-**30** = 2.5; IC_{50} *rac*-**29**/IC_{50} *rac*-**28** = 3.7). Also, for a given location of the substituent, the activity is greater for the fluoro derivative than for the methyl derivative (for example, IC_{50} *rac*-**27**/IC_{50} *rac*-**28** = 1.5). The more active compound prepared, *rac*-**28**, is about 9-fold more active than (−)-huperzine A. Although the eutomer of compounds **19**, **20**, **28**, and **30** is always the (−)-enantiomer, as in the case of huperzine A, it is worth noting that their absolute configurations[17] are opposite to that of (−)-huperzine A. The eutomers of these hybrid compounds are roughly 2-fold more active than their racemic mixtures, and thus, (−)-**28** is about 21-fold more active than (−)-huperzine A. Moreover, the more active AChE inhibitors of this series proved to be quite selective in

inhibiting AChE as compared with BChE. Thus, *rac*-**27**−**31** showed inhibitory activities toward AChE that were 17−36-fold greater than those observed in inhibiting BChE. A still greater selectivity was observed for the eutomers of two of these compounds [(−)-**28** and (−)-**30**] which were respectively 40- and 77-fold more active in inhibiting AChE than BChE. Most of the tested compounds [for example, *rac*-**19**, (−)-**19**, *rac*-**20**, (−)-**20**, *rac*-**21**, *rac*-**28**, (−)-**28**, *rac*-**29**, (−)-**30**, and *rac*-**31**] proved to be also much more active than THA in reversing the neuromuscular blockade.

Molecular modeling of these compounds with AChE from *T. californica* provides a basis to suggest that they interact as truly THA−huperzine A hybrids: the 4-aminoquinoline substructure of (−)-**19** occupies the same position of the corresponding subunit in THA, while the bicyclo[3.3.1]nonadiene substructure of (−)-**19** occupies roughly the same position of the corresponding subunit in (−)-huperzine A, a fact that is only possible for the levorotatory eutomers of hybrids **19**−**31** and (−)-huperzine A. Even though caution is needed because the AChE from *T. californica* is somewhat different from human AChE and because of the approximations of the computational model, the results herein described provide a basis to pursue our efforts to develop compounds with improved inhibitory activity.

Experimental Section

Chemistry. General Methods. Melting points were determined in open capillary tubes with a MFB 595010M Gallenkamp melting point apparatus. ^{1}H NMR spectra were recorded at 500 MHz on a Varian VXR 500 spectrometer, and ^{13}C NMR spectra were recorded at 75.4 or 50.3 MHz on a Varian Gemini 300 or 200 spectrometer. The chemical shifts are reported in ppm (δ scale) relative to internal TMS, and coupling constants are reported in hertz (Hz). COSY ^{1}H/^{1}H experiments were performed using standard procedures, while COSY ^{1}H/^{13}C were performed using the HMQC sequence with an indirect detection probe. For the ^{13}C and ^{1}H NMR data of oxaadamantanols **11** and mesylates **12**, and of compounds *rac*-**21**−**31**, see Tables 1, 3, 2, and 4, respectively, of Supporting Information. For the NMR data of the rest of compounds, enones *rac*-**13** and compound **38**, see the Experimental Section. IR spectra were run on a FT/IR Perkin-Elmer model 1600 spectrophotometer. Absorption values are expressed as wavenumbers (cm^{-1}). Mass spectra were recorded on a Hewlett-Packard HP-5988A spectrometer (electron impact). Optical rotations were measured on a Perkin-Elmer model 241 polarimeter. The specific rotation has not been corrected for the presence of solvent of crystallization. Chiral HPLC analyses were performed on a Waters model 600 liquid chromatograph provided with a Waters model 486 variable λ detector, using a CHIRALCEL OD-H column (25 × 0.46 cm) containing the chiral stationary phase cellulose tris(3,5-dimethylphenylcarbamate). Conditions A: mixture of hexane/EtOH in the ratio of 75:25 as eluent, flow 0.20 mL/min, λ = 235 nm. Chiral medium-pressure liquid chromatography (chiral MPLC) separation was carried out on equipment which consisted of a pump (Büchi 688), a variable λ UV detector (Büchi), and a column (25 × 2.5 cm) containing microcrystalline cellulose triacetate (15−25 μm) as the chiral stationary phase. Column chromatography was performed on silica gel 60 AC.C. (70−200 mesh, SDS, ref 2100027). For the TLC, aluminum-backed sheets with silica gel 60 F_{254} (Merck, ref 1.05554) were used. $CeCl_3 \cdot 7H_2O$ and *t*-BuLi were purchased from Fluka, while lithium, allyl phenyl ether, vinyl bromide, methanesulfonyl chloride, and $AlCl_3$ were purchased from Aldrich. Anhydrous THF and Et_2O were distilled over sodium, and anhydrous CH_2Cl_2 was distilled over P_2O_5. Analytical grade solvents were used for recrystallizations, while pure synthesis solvents were used in extractions and column chromatography. Pure-for-synthesis 1,2-dichloroethane and 1,2-dibromoethane were also used. Et_3N was distilled over KOH. Aminobenzonitriles **14** and **18** were purchased from Fluka and ABCR, respectively, while **15**−**17** were prepared according to literature procedures.[50−52] Elemental analyses were carried out at the Microanalysis Service of the Centro de Investigación y Desarrollo, C.I.D., Barcelona, Spain, and are within ±0.4% of the theoretical values.

3-Methyl-2-oxa-1-adamantanol (11a). $CeCl_3 \cdot 7H_2O$ (3.80 g, 10.2 mmol) was dried at 160 °C/1 Torr for 16 h and suspended in anhydrous THF (50 mL). The suspension was stirred at room temperature for 2 h, cooled to −78 °C, and treated with a solution of MeMgBr (1 M solution in pentane, 8.10 mL, 8.10 mmol). The mixture was stirred at −78 °C for 1 h and treated dropwise with a solution of diketone **10** (0.50 g, 3.29 mmol) in anhydrous THF (10 mL). The reaction mixture was stirred at −78 °C for 1 h, allowed to warm to room temperature over 3 h, stirred at room temperature for 12 h, and treated with saturated aqueous NH_4Cl (20 mL). The organic layer was separated, and the aqueous one was extracted with CH_2Cl_2 (3 × 100 mL). The combined organic layers were dried with Na_2SO_4 and evaporated under reduced pressure. Sublimation of the resulting white solid residue (0.79 g) at 80 °C/0.5 Torr afforded pure oxaadamantanol **11a** (0.50 g, 91% yield).

3-Ethyl-2-oxa-1-adamantanol (11b). This compound was prepared from $CeCl_3 \cdot 7H_2O$ (3.80 g, 10.2 mmol), EtMgBr (1 M solution in pentane, 8.10 mL, 8.10 mmol), and diketone **10** (0.50 g, 3.29 mmol) in a manner similar to that described for **11a**. Sublimation of the resulting white solid residue (0.85 g) at 80 °C/0.5 Torr afforded pure oxaadamantanol **11b** (0.51 g, 85% yield).

3-Vinyl-2-oxa-1-adamantanol (11c). A cooled (−78 °C) solution of vinyl bromide (0.50 mL, 758 mg, 7.09 mmol) in anhydrous Et_2O (16 mL) was treated dropwise over a 10-min period with a solution of *t*-BuLi (1.5 M solution in pentane, 9.0 mL, 13.5 mmol) and stirred at −78 °C for 30 min. To the resulting solution was added a solution of diketone **10** (0.50 g, 3.29 mmol) in anhydrous THF (15 mL) dropwise. The reaction mixture was stirred at −78 °C for 30 min, allowed to warm to 0 °C over 3 h, diluted with anhydrous THF (5 mL), stirred at 0 °C for an additional 30-min period, quenched with saturated aqueous NH_4Cl (10 mL), and diluted with water (20 mL). The organic layer was separated, and the aqueous one was extracted with CH_2Cl_2 (4 × 30 mL). The combined organic layers were dried with Na_2SO_4 and evaporated under reduced pressure to give a white solid residue (420 mg), which was submitted to column chromatography [silica gel (21 g), hexane/AcOEt mixtures]. On elution with hexane/AcOEt (85:15), oxaadamantanol **11c** (350 mg, 59% yield) was isolated: mp 84−87 °C after recrystallization from hexane; IR 3361 (OH). Anal. ($C_{11}H_{16}O_2$) C, H.

3-Isopropyl-2-oxa-1-adamantanol (11e). This compound was prepared from $CeCl_3 \cdot 7H_2O$ (5.10 g, 13.7 mmol), *i*-PrLi (0.12 M solution in pentane, 100 mL, 12.0 mmol),[53] and diketone **10** (1.00 g, 6.58 mmol) in a manner similar to that described for **11a**. Sublimation of the resulting white solid residue (0.90 g) at 100 °C/1 Torr afforded pure oxaadamantanol **11e** (0.75 g, 58% yield): mp 129−131 °C after recrystallization from CH_2Cl_2; IR 3313 (OH). Anal. ($C_{12}H_{20}O_2$) C, H.

3-Allyl-2-oxa-1-adamantanol (11f). A cooled (−15 °C) suspension of lithium (9.94 g, 1.43 at.-g) in anhydrous THF (250 mL) was treated dropwise over a 45-min period with a solution of allyl phenyl ether (16.2 mL, 15.9 g, 118.3 mmol) in anhydrous Et_2O (60 mL).[54] The cooling bath was removed, and the mixture was stirred for 15 min, cooled again to −15 °C, and treated dropwise over a period of 30 min with a solution of diketone **10** (12.0 g, 78.9 mmol) in anhydrous THF (240 mL). The reaction mixture was stirred at −15 °C for 30 min, and then it was treated with saturated aqueous NH_4Cl (200 mL). The organic layer was separated, and the aqueous one was extracted with CH_2Cl_2 (5 × 150 mL). The combined organic extracts were washed with 1 N NaOH (4 × 100 mL), dried with Na_2SO_4, and evaporated under reduced pressure. Subli-

mation of the resulting solid residue (11.4 g) at 75 °C/3 Torr afforded pure oxaadamantanol **11f** (8.74 g, 57% yield): mp 100−101 °C; IR 3323 (OH). Anal. ($C_{12}H_{18}O_2$) C, H.

3-*tert*-Butyl-2-oxa-1-adamantanol (11h). This compound was prepared from $CeCl_3 \cdot 7H_2O$ (30.4 g, 81.6 mmol), *t*-BuLi (1.5 M solution in pentane, 54.0 mL, 81.0 mmol), and diketone **10** (4.00 g, 26.3 mmol) in a manner similar to that described for **11a**. Sublimation of the resulting white solid residue (3.50 g) at 80 °C/0.5 Torr afforded pure oxaadamantanol **11h** (3.00 g, 54% yield): mp 125−127 °C after recrystallization from hexane; IR 3323 (OH). Anal. ($C_{13}H_{22}O_2$) C, H.

3-(3,3-Dimethylbutyl)-2-oxa-1-adamantanol (11j). To a cooled (0 °C) solution of *t*-BuLi (1.5 M solution in pentane, 10 mL, 15.0 mmol) was added dropwise over a 30-min period a solution of diketone **10** (1.00 g, 6.58 mmol) in anhydrous THF (20 mL). The mixture was stirred at 0 °C for 30 min and treated with saturated aqueous NH_4Cl (30 mL). The organic layer was separated, and the aqueous one was extracted with Et_2O (4 × 100 mL). The combined organic layers were dried with Na_2SO_4 and evaporated under reduced pressure to give a white solid residue (1.10 g), which was submitted to column chromatography [silica gel (25 g), hexane/AcOEt mixtures]. On elution with hexane/AcOEt (70:30), oxaadamantanol **11j** (0.70 g, 45% yield) was isolated: mp 148−150 °C after sublimation at 100 °C/1 Torr; IR 3314 (OH); EI-MS *m*/*z* 239 ($M^+ + 1$, 3), 238 ($M^{\bullet+}$, 19), 223 ($M^+ - CH_3$, 1), 221 ($M^+ - OH$, 2), 206 ($M^{\bullet+} - CH_3 - OH$, 2), 153 ($M^+ - C_6H_{13}$, 72), 136 ($M^{\bullet+} - C_6H_{13} - OH$, 9). Anal. ($C_{15}H_{26}O_2$) C, H.

General Procedure for the Preparation of Mesylates 12 from 2-Oxaadamantanols 11. A solution of the alcohol **11** (1 mmol) and anhydrous Et_3N (1.4 mmol) in anhydrous CH_2Cl_2 (5 mL) was cooled to −10 °C. Methanesulfonyl chloride (1.6 mmol) was added dropwise over a period of 10 min, and the reaction mixture was stirred at −10 °C for 30 min. The mixture was poured into a mixture of 2 N HCl (5 mL) and crushed ice. The organic layer was separated, and the aqueous one was extracted with CH_2Cl_2 (4 × 20 mL). The combined organic extracts were washed with saturated aqueous $NaHCO_3$ (25 mL) and brine (25 mL), dried with Na_2SO_4, and evaporated under reduced pressure to afford the corresponding mesylate **12**.

3-Vinyl-2-oxa-1-adamantyl Methanesulfonate (12c). This compound was prepared according to the procedure described above: yield 0.26 g, 91%; IR 1357, 1166 (SO_2). Anal. ($C_{12}H_{18}O_4S \cdot 2/3H_2O$) C, H, S.

3-Isopropyl-2-oxa-1-adamantyl Methanesulfonate (12e). This compound was prepared according to the procedure described above: yield 0.36 g, 81%; IR 1350, 1184 (SO_2). Anal. ($C_{13}H_{22}O_4S$) C, H, S.

3-Allyl-2-oxa-1-adamantyl Methanesulfonate (12f). This compound was prepared according to the procedure described above: yield 7.97 g, 98%; IR 1358, 1180 (SO_2). Anal. ($C_{13}H_{20}O_4S$) C, H, S.

3-*tert*-Butyl-2-oxa-1-adamantyl Methanesulfonate (12h). This compound was prepared according to the procedure described above: yield 0.38 g, 89%; IR 1356, 1178 (SO_2). Anal. ($C_{14}H_{24}O_4S$) C, H, S.

***rac*-7-Isopropylbicyclo[3.3.1]non-6-en-3-one (*rac*-13e).** A suspension of mesylate **12e** (0.25 g, 0.91 mmol) and silica gel (2 g) in CH_2Cl_2 (15 mL) was stirred at room temperature for 4 h. After concentrating at reduced pressure, the resulting solid residue was submitted to column chromatography through silica gel (25 g) using mixtures of hexane/AcOEt as eluent. On elution with hexane/AcOEt (75:25), enone *rac*-**13e** (70 mg, 43% yield) was obtained, and on elution with hexane/AcOEt (60:40), oxaadamantanol **11e** (20 mg, 11% yield) was isolated. *rac*-**13e**: mp 38−40 °C after sublimation at 60 °C/0.5 Torr; IR 1701 (C=O); ^{1}H NMR ($CDCl_3$) δ 0.92 (d, J = 7.0 Hz, 3 H) and 0.93 (d, J = 7.0 Hz, 3 H) [CH(CH_3)$_2$], 1.84 (br. d, J = 17.5 Hz, 1 H, 8-H_{endo}), 1.93 (dm, J = 12.5 Hz, 1 H) and 1.98 (dm, $J \approx$ 12.5 Hz, 1 H) (9-H_{syn} and 9-H_{anti}), 2.08 [heptet, J = 7.0 Hz, 1 H, CH(CH_3)$_2$], 2.22 (dddd, J = 15.5 Hz, $J' = J'' = J'''$ = 2.0 Hz, 1 H, 2-H_{endo}), 2.28 (dddd, J = 14.5 Hz, $J' \approx J'' \approx J''' \approx$ 2.5 Hz, 1 H, 4-H_{endo}), superimposes in part 2.32 (br. dd, J = 17.5 Hz, J' = 5.5 Hz, 1 H, 8-H_{exo}), 2.41 (dd, J = 14.5 Hz, J' = 4.0 Hz, 1 H, 4-H_{exo}), 2.48 (dd, J = 15.5 Hz, J' = 6.5 Hz, 1 H, 2-H_{exo}), 2.57 (m, 1 H, 1-H), 2.65 (m, 1 H, 5-H), 5.41 (dm, J = 5.7 Hz, 1 H, 6-H); ^{13}C NMR ($CDCl_3$) δ 21.1 (CH_3) and 21.5 (CH_3) [CH(CH_3)$_2$], 30.0 (CH, C1), 30.5 (CH_2, C9), 30.8 (CH, C5), 33.2 (CH_2, C8), 34.6 [CH, CH(CH_3)$_2$], 46.7 (CH_2, C4), 49.0 (CH_2, C2), 122.0 (CH, C6), 142.4 (C, C7), 212.0 (C, C3). Anal. ($C_{12}H_{18}O$) C, H.

***rac*-7-Allylbicyclo[3.3.1]non-6-en-3-one (*rac*-13f).** A suspension of mesylate **12f** (7.50 g, 27.6 mmol) and silica gel (7.50 g) in CH_2Cl_2 (75 mL) was stirred at room temperature for 3 h and concentrated at reduced pressure. The resulting solid residue was submitted to column chromatography through silica gel (100 g) using mixtures of hexane/AcOEt as eluent. On elution with hexane/AcOEt (90:10), enone *rac*-**13f** (2.44 g, 50% yield) was isolated, and on elution with hexane/AcOEt (80:20), oxaadamantanol **11f** (1.13 g, 21% yield) was obtained. *rac*-**13f**: bp 75 °C/1 Torr; IR 1697 (C=O); ^{1}H NMR ($CDCl_3$) δ 1.83 (br. d, J = 18.0 Hz, 1 H, 8-H_{endo}), 1.94 (dm, J = 13.0 Hz, 1 H, 9-H_{anti}), 1.99 (dddd, J = 13.0 Hz, J' = 5.0 Hz, J'' = 2.5 Hz, J''' = 1.0 Hz, 1 H, 9-H_{syn}), 2.26 (dddd, J = 15.5 Hz, $J' = J'' = J'''$ = 2.0 Hz, 1 H, 2-H_{endo}), 2.32 (dddd, J = 14.5 Hz, $J' \approx J'' \approx J''' \approx$ 2.0 Hz, 1 H, 4-H_{endo}), superimposes in part ca. 2.34 (br. dd, J = 18.0 Hz, J' = 5.0 Hz, 1 H, 8-H_{exo}), 2.43 (dd, J = 14.5 Hz, J' = 4.5 Hz, 1 H, 4-H_{exo}), 2.50 (dddd, J = 15.5 Hz, J' = 6.5 Hz, $J'' = J'''$ = 1.0 Hz, 1 H, 2-H_{exo}), 2.58 (m, 1 H, 1-H), 2.62 (br. d, J = 7.0 Hz, 2 H, CH_2−CH=CH_2), 2.69 (br. s, 1 H, 5-H), 4.99 (dm, $J \approx$ 17.5 Hz, 1 H, CH_2−CH=CH_{trans}), 5.00 (dm, $J \approx$ 10.0 Hz, 1 H, CH_2−CH=CH_{cis}), 5.48 (ddt, J = 6.0 Hz, J' = 2.3 Hz, J'' = 1.2 Hz, 1 H, 6-H), 5.70 (dm, $J \approx$ 18.0 Hz, 1 H, CH_2−CH=CH_2); ^{13}C NMR ($CDCl_3$) δ 30.1 (CH, C1), 30.3 (CH_2, C9), 31.0 (CH, C5), 35.5 (CH_2, C8), 41.5 (CH_2, CH_2−CH=CH_2), 46.4 (CH_2, C4), 49.0 (CH_2, C2), 116.0 (CH_2, CH_2−CH=CH_2), 125.3 (CH, C6), 135.0 (C, C7), 136.1 (CH, CH_2-CH=CH_2), 212.1 (C, C3). Anal. ($C_{12}H_{16}O$) C, H.

***rac*-7-*tert*-Butylbicyclo[3.3.1]non-6-en-3-one (*rac*-13h).** A stirred suspension of mesylate **12h** (0.32 g, 1.11 mmol) in hexane (50 mL) was heated under reflux for 30 min; to the resulting mixture was added H_2O (20 mL). The organic phase was separated and washed successively with saturated aqueous $NaHCO_3$ (50 mL) and brine (50 mL), dried with Na_2SO_4, and evaporated under reduced pressure to afford the enone *rac*-**13h** (0.17 g, 80% yield) as a white solid: mp 60−62 °C after sublimation at 70 °C/1 Torr; IR 1699 (C=O); ^{1}H NMR ($CDCl_3$) δ 0.95 [s, 9 H, C(CH_3)$_3$], 1.91 (dm, J = 12.5 Hz, 1 H) and 1.96 (dm, $J \approx$ 12.5 Hz, 1 H) (9-H_{syn} and 9-H_{anti}), 1.97 (br. d, J = 17.5 Hz, 1 H, 8-H_{endo}), 2.21 (dddd, J = 15.5 Hz, $J' = J'' = J'''$ = 2.0 Hz, 1 H, 2-H_{endo}), 2.28 (dddd, J = 14.5 Hz, $J' \approx J'' \approx J''' \approx$ 2.5 Hz, 1 H, 4-H_{endo}), 2.33 (ddm, J = 17.5 Hz, J' = 6.0 Hz, 1 H, 8-H_{exo}), 2.41 (dd, J = 14.5 Hz, J' = 4.2 Hz, 1 H, 4-H_{exo}), 2.47 (dddd, J = 15.5 Hz, J' = 6.5 Hz, $J'' = J'''$ = 1.0 Hz, 1 H, 2-H_{exo}), 2.58 (m, 1 H, 1-H), 2.68 (m, 1 H, 5-H), 5.46 (dm, J = 5.7 Hz, 1 H, 6-H); ^{13}C NMR ($CDCl_3$) δ 28.9 [CH_3, C(CH_3)$_3$], 30.1 (CH, C1), 30.2 (CH_2, C9), 30.9 (CH, C5), 32.0 (CH_2, C8), 35.1 [C, C(CH_3)$_3$], 46.8 (CH_2, C4), 48.8 (CH_2, C2), 121.1 (CH, C6), 144.3 (C, C7), 211.9 (C, C3). Anal. ($C_{13}H_{20}O$) C, H.

General Procedure for the Preparation of Compounds *rac*-21−31 from Enones *rac*-13 and 2-Aminobenzonitriles 14−18. To a suspension of anhydrous $AlCl_3$ (2 mmol) and 2-aminobenzonitrile **14**−**18** (1.4 mmol) in 1,2-dichloroethane (2 mL) was added a solution of enone *rac*-**13** (1 mmol) in 1,2-dichloroethane (12 mL) dropwise. The reaction mixture was stirred under reflux for 7 h, allowed to cool to room temperature, diluted with water (7 mL) and THF (7 mL), made basic by addition of 5 N NaOH, and stirred at room temperature for 30 min. The organic solvents were removed under reduced pressure, and the residue was filtered. The solid residue was submitted to column chromatography [silica gel (12 g), hexane/AcOEt/MeOH mixtures] to give *rac*-**21**−**31**. A solution of *rac*-**21**−**31** in MeOH was treated with a solution of HCl (0.55 N solution in Et_2O, 3 equiv), and the solvent was evaporated to give *rac*-**21**−**31**·HCl, which were recrystallized.

***rac*-12-Amino-6,7,10,11-tetrahydro-9-propyl-7,11-methanocycloocta[*b*]quinoline Hydrochloride (*rac*-21·HCl).**

This compound was prepared according to the procedure described above. On elution with AcOEt/MeOH (70:30), *rac*-**21** (2.82 g, 98% yield) was isolated. Subsequent treatment with a solution of HCl (0.55 N solution in Et_2O, 3 equiv), evaporation, and recrystallization of the resulting solid from MeOH/H_2O (1:1) afforded pure *rac*-**21**·HCl (37% overall yield): mp 331−333 °C; IR 3500−2000 (max at 3320, 3146, 3071, 3029, 2943, 2900, 2871, 2820, 2686, 2371) (CH, NH, NH^+), 1662 and 1586 (ar-C−C and ar-C−N). Anal. ($C_{19}H_{22}N_2$·HCl) C, H, N, Cl.

***rac*-12-Amino-9-isopropyl-6,7,10,11-tetrahydro-7,11-methanocycloocta[*b*]quinoline Hydrochloride (*rac*-22·HCl).** This compound was prepared according to the procedure described above, with a reaction time of 12 h. On elution with hexane/AcOEt (25:75), *rac*-**22** (0.31 g, quantitative yield) was isolated. Subsequent treatment with a solution of HCl (0.55 N solution in Et_2O, 3 equiv), evaporation, and recrystallization of the resulting solid from MeOH/AcOEt (1:4) afforded pure *rac*-**22**·HCl (48% overall yield): mp > 300 °C dec; IR 3500−2500 (max at 3327, 3149, 2958, 2929, 2895, 2825, 2691) (CH, NH, NH^+), 1656 and 1587 (ar-C−C and ar-C−N). Anal. ($C_{19}H_{22}N_2$·HCl) C, H, N, Cl.

***rac*-9-Allyl-12-amino-6,7,10,11-tetrahydro-7,11-methanocycloocta[*b*]quinoline Hydrochloride (*rac*-23·HCl).** This compound was prepared according to the procedure described above, but using 1 equiv of $AlCl_3$ and 2 equiv of 2-aminobenzonitrile and a reaction time of 2.5 h. After the basic treatment, the organic solvent was removed under reduced pressure, and the aqueous residue was extracted with AcOEt (4 × 100 mL). The combined organic extracts were dried with Na_2SO_4 and evaporated to give an oily residue, which was submitted to column chromatography. On elution with hexane/AcOEt (40:60), *rac*-**23** (0.38 g, 48% yield) was isolated. Subsequent treatment with a solution of HCl (0.55 N solution in Et_2O, 3 equiv), evaporation, and recrystallization of the resulting solid from AcOEt/MeOH (3:2) afforded pure *rac*-**23**·HCl (31% overall yield): mp > 300 °C dec; IR 3500−2000 (max at 3328, 3141, 3083, 3024, 2929, 2893, 2857, 2820, 2690, 2369) (CH, NH, NH^+), 1664 and 1585 (ar-C−C and ar-C−N). Anal. ($C_{19}H_{20}N_2$·HCl) C, H, N, Cl.

***rac*-12-Amino-9-butyl-6,7,10,11-tetrahydro-7,11-methanocycloocta[*b*]quinoline Hydrochloride (*rac*-24·HCl).** This compound was prepared according to the procedure described above. On elution with AcOEt/MeOH (70:30), *rac*-**24** (2.40 g, 72% yield) was isolated. Subsequent treatment with a solution of HCl (0.55 N solution in Et_2O, 3 equiv), evaporation, and recrystallization of the resulting solid from MeOH/H_2O (2:3) afforded pure *rac*-**24**·HCl (29% overall yield): mp 328−330 °C; IR 3500−2000 (max at 3316, 3146, 3073, 3049, 2939, 2902, 2878, 2823, 2692, 2390) (CH, NH, NH^+), 1660 and 1587 (ar-C−C and ar-C−N). Anal. ($C_{20}H_{24}N_2$·HCl) C, H, N, Cl.

***rac*-12-Amino-9-*tert*-butyl-6,7,10,11-tetrahydro-7,11-methanocycloocta[*b*]quinoline Hydrochloride (*rac*-25·HCl).** This compound was prepared according to the procedure described above, with a reaction time of 12 h. On elution with hexane/AcOEt (30:70), *rac*-**25** (2.70 g, 89% yield) was isolated. Subsequent treatment with a solution of HCl (0.55 N solution in Et_2O, 3 equiv), evaporation, and recrystallization of the resulting solid from MeOH/H_2O (1:5) afforded *rac*-**25**·HCl·H_2O (49% overall yield): mp > 300 °C dec; IR 3500−2500 (max at 3324, 3191, 3143, 2961, 2888, 2853, 2685) (CH, NH, NH^+), 1639 and 1587 (ar-C−C and ar-C−N). Anal. ($C_{20}H_{24}N_2$·HCl·H_2O) C, H, N, Cl.

***rac*-12-Amino-9-phenyl-6,7,10,11-tetrahydro-7,11-methanocycloocta[*b*]quinoline Hydrochloride (*rac*-26·HCl).** This compound was prepared according to the procedure described above. On elution with AcOEt/MeOH (90:10), *rac*-**26** (0.73 g, 50% yield) was isolated. Subsequent treatment with a solution of HCl (0.55 N solution in Et_2O, 3 equiv), evaporation, and recrystallization of the resulting solid from AcOEt/MeOH (1:1) afforded *rac*-**26**·HCl·5/4H_2O (35% overall yield): mp 206−207 °C; IR 3500−2500 (max at 3330, 3200, 3025, 2937, 2898, 2812, 2687) (CH, NH, NH^+), 1647 and 1589 (ar-C−C and ar-C−N). Anal. ($C_{22}H_{20}N_2$·HCl·5/4H_2O) C, H, N, Cl.

***rac*-12-Amino-6,7,10,11-tetrahydro-3,9-dimethyl-7,11-methanocycloocta[*b*]quinoline Hydrochloride (*rac*-27·HCl).** This compound was prepared according to the procedure described above, with a reaction time of 12 h. On elution with hexane/AcOEt (20:80), *rac*-**27** (3.20 g, 91% yield) was isolated. Subsequent treatment with a solution of HCl (0.55 N solution in Et_2O, 3 equiv), evaporation, and recrystallization of the resulting solid from MeOH/AcOEt (1:4) afforded *rac*-**27**·HCl·5/3H_2O (48% overall yield): mp 321−323 °C dec; IR 3500−2500 (max at 3336, 3189, 2927, 2875, 2825, 2699) (CH, NH, NH^+), 1650 and 1592 (ar-C−C and ar-C−N). Anal. ($C_{18}H_{20}N_2$·HCl·5/3H_2O) C, H, N, Cl.

***rac*-12-Amino-3-fluoro-6,7,10,11-tetrahydro-9-methyl-7,11-methanocycloocta[*b*]quinoline Hydrochloride (*rac*-28·HCl).** This compound was prepared according to the procedure described above, with a reaction time of 7 h. On elution with hexane/AcOEt (30:70), *rac*-**28** (2.27 g, 74% yield) was isolated. Subsequent treatment with a solution of HCl (0.55 N solution in Et_2O, 3 equiv), evaporation, and recrystallization of the resulting solid from MeOH/H_2O (1:3) afforded *rac*-**28**·HCl·2/3H_2O (42% overall yield): mp 220−222 °C dec; IR 3700−2400 (max at 3334, 3026, 3013, 2926, 2826, 2701) (CH, NH, NH^+), 1651 and 1591 (ar-C−C and ar-C−N). Anal. ($C_{17}H_{17}FN_2$·HCl·2/3H_2O) C, H, N, Cl.

Preparative Resolution of *rac*-28 by Chiral MPLC: (+)-(7*R*,11*R*)-28 and (−)-(7*S*,11*S*)-28. The chromatographic resolution of *rac*-**28** was carried out by using MPLC equipment provided with a column (25 × 2.5 cm) containing microcrystalline cellulose triacetate (15−25 μm), pretreated with a 0.1% solution of Et_3N in EtOH, as the chiral stationary phase. The sample of *rac*-**28** (4.08 g) was introduced as free base in eight portions (1 × 120 mg + 3 × 360 mg + 4 × 720 mg) using 96% EtOH (2 mL/min) as the sole eluent and solvent. The chromatographic fractions (5 mL) were analyzed by chiral HPLC under conditions A [(−)-**28**, t_R = 22.02 min, k'_1 = 1.17; (+)-**28**, t_R = 25.00 min, k'_2 = 1.47, α = 1.25, Res. = 1.70] and combined conveniently. In this way, (−)-**28** (250 mg, 68% ee) and (+)-**28** (360 mg, 69% ee) were obtained. The remaining product consisted of mixtures of both enantiomers with lower ee's.

A solution of (−)-**28** (250 mg, 68% ee) in MeOH (50 mL) was treated with active charcoal for 15 min and filtered through Celite. The filtrate was evaporated at reduced pressure, and the resulting solid (200 mg) was taken up in MeOH (6 mL) and treated with excess 0.55 N HCl in Et_2O (5 mL). The organic solvents were removed under reduced pressure, and the residue (240 mg) was recrystallized from acetonitrile/MeOH (4:1) (10 mL) to afford (−)-**28**·HCl·3/4H_2O {110 mg, $[\alpha]^{20}_D = -301$ (c = 1.00, MeOH), 95% ee by chiral HPLC on the liberated base}: mp 242−243 °C; IR 3500−2500 (max at 3464, 3307, 3120, 3029, 2930, 2884, 2834, 2749, 2704, 2681) (CH, NH, NH^+), 1650 and 1588 (ar-C−C and ar-C−N). Anal. ($C_{17}H_{17}FN_2$·HCl·3/4H_2O) C, H, N.

A solution of (+)-**28** (360 mg, 69% ee) in MeOH (50 mL) was treated with active charcoal for 15 min and filtered through Celite. The filtrate was evaporated at reduced pressure, and the resulting solid (310 mg) was taken up in an acetonitrile/MeOH mixture in the ratio of 2:1 (15 mL) and treated with excess 0.55 N HCl in Et_2O (7 mL). The volatile materials were removed in vacuo, and the residue (340 mg) was recrystallized from acetonitrile/MeOH (4:1) (15 mL) to afford a brown solid consisting of (+)-**28**·HCl·H_2O (160 mg, 35% ee). Evaporation of the mother liquors gave a brown solid residue which was decolorized with active charcoal for 15 min and filtered through Celite, and the filtrate was concentrated in vacuo to give a solid (130 mg) which was recrystallized from a mixture of acetonitrile/MeOH (4:1) (5 mL) to afford, after drying, pure (+)-**28**·HCl·H_2O {40 mg, $[\alpha]^{20}_D = +290$ (c = 1.00, MeOH), 99% ee by chiral HPLC on the liberated base}: mp 236−238 °C; IR 3500−2500 (max at 3343, 3195, 2934, 2910, 2863, 2827, 2696) (CH, NH, NH^+), 1664 and 1592 (ar-C−C and ar-C−N). Anal. ($C_{17}H_{17}FN_2$·HCl·H_2O) C, H, N.

***rac*-12-Amino-1-fluoro-6,7,10,11-tetrahydro-9-methyl-7,11-methanocycloocta[*b*]quinoline Hydrochloride (*rac*-29·HCl).** This compound was prepared according to the

procedure described above, with a reaction time of 1 h. On elution with AcOEt/MeOH (90:10), *rac*-**29** (1.18 g, 66% yield) was isolated. Subsequent treatment with a solution of HCl (0.55 N solution in Et_2O, 3 equiv), evaporation, and recrystallization of the resulting solid from AcOEt/MeOH (1:1) afforded *rac*-**29**·HCl (23% overall yield): mp 268 °C dec; IR 3700−2000 (max at 3408, 3161) (CH, NH, NH^+), 1639 and 1595 (ar-C−C and ar-C−N). Anal. ($C_{17}H_{17}FN_2$·HCl) C, H, N, Cl.

***rac*-12-Amino-9-ethyl-6,7,10,11-tetrahydro-3-methyl-7,11-methanocycloocta[*b*]quinoline Hydrochloride (*rac*-30·HCl).** This compound was prepared according to the procedure described above. On elution with hexane/AcOEt (10:90), *rac*-**30** (0.68 g, 25% yield) was isolated. Subsequent treatment with a solution of HCl (0.55 N solution in Et_2O, 3 equiv), evaporation, and recrystallization of the resulting solid from acetonitrile/H_2O (1:1) afforded *rac*-**30**·HCl·3/2H_2O (15% overall yield): mp 208−210 °C; IR 3500−2500 (max at 3341, 3204, 3088, 3053, 2972, 2925, 2780, 2688) (CH, NH, NH^+), 1667 and 1591 (ar-C−C and ar-C−N). Anal. ($C_{19}H_{22}N_2$·HCl·3/2H_2O) C, H, N, Cl.

Preparative Resolution of *rac*-30 by Chiral MPLC: (+)-(7*R*,11*R*)-30 and (−)-(7*S*,11*S*)-30. The chromatographic resolution of *rac*-**30** was carried out by using MPLC equipment provided with a column (25 × 2.5 cm) containing microcrystalline cellulose triacetate (15−25 μm), pretreated with a 0.1% solution of Et_3N in EtOH, as the chiral stationary phase. The sample of *rac*-**30** (800 mg) was introduced as free base in five portions (3 × 120 mg + 2 × 220 mg) using 96% EtOH (2 mL/min) as the sole eluent and solvent. The chromatographic fractions (5 mL) were analyzed by chiral HPLC under conditions A [(−)-**30**, t_R = 20.57 min, k'_1 = 0.33; (+)-**30**, t_R = 23.38 min, k'_2 = 0.51, α = 1.55, Res. = 1.68] and combined conveniently. In this way, (−)-**30** (340 mg, 74% ee) and (+)-**30** (220 mg, 94% ee) were obtained. The remaining product consisted of mixtures of both enantiomers with lower ee's.

A solution of (−)-**30** (340 mg, 74% ee) in MeOH (10 mL) was treated with excess 0.55 N HCl in Et_2O (11 mL), and the organic solvents were removed under reduced pressure. The residue (350 mg) was recrystallized from acetonitrile/MeOH (13:2) (15 mL). The resulting white solid (100 mg) was separated, and the mother liquors were treated with active charcoal and concentrated in vacuo. The residue was recrystallized from acetonitrile/MeOH (5:1) (6 mL). The crystalline white solid obtained (30 mg) was combined with the first one and recrystallized from acetonitrile/MeOH (4:1) (5 mL) to afford (−)-**30**·HCl·1/4H_2O {90 mg, $[\alpha]^{20}_D$ = −290 (c = 1.00, MeOH), 97% ee by chiral HPLC on the liberated base}: mp > 300 °C dec; IR 3500−2500 (max at 3335, 3176, 2966, 2925, 2901, 2829, 2698) (CH, NH, NH^+), 1669 and 1591 (ar-C−C and ar-C−N). Anal. ($C_{19}H_{22}N_2$·HCl·1/4H_2O) C, H, N.

Similarly, from (+)-**30** (220 mg, 94% ee), (+)-**30**·HCl·1/4H_2O {120 mg, $[\alpha]^{20}_D$ = +284 (c = 1.10, MeOH), 96% ee by chiral HPLC on the liberated base} was obtained: mp > 300 °C dec; IR 3500−2500 (max at 3332, 3157, 2962, 2923, 2856, 2689) (CH, NH, NH^+), 1666 and 1590 (ar-C−C and ar-C−N). Anal. ($C_{19}H_{22}N_2$·HCl·1/4H_2O) C, H, N.

***rac*-12-Amino-9-ethyl-6,7,10,11-tetrahydro-1-methyl-7,11-methanocycloocta[*b*]quinoline Hydrochloride (*rac*-31·HCl).** This compound was prepared according to the procedure described above, but carrying out the reaction in 1,2-dibromoethane for 18 h. On elution with AcOEt/MeOH (80:20), *rac*-**31** (1.76 g, 65% yield) was isolated. Subsequent treatment with a solution of HCl (0.55 N solution in Et_2O, 3 equiv), evaporation, and recrystallization of the resulting solid from MeOH/AcOEt/Et_2O (1:5:3) afforded *rac*-**31**·HCl·1/2H_2O (41% overall yield): mp 282−283 °C; IR 3500−2500 (max at 3310, 3177, 3091, 3034, 2966, 2932, 2899, 2864, 2750) (CH, NH, NH^+), 1650 and 1588 (ar-C−C and ar-C−N). Anal. ($C_{19}H_{22}N_2$·HCl·1/2H_2O) C, H, N, Cl.

***N,N'*-Bis(2-cyano-3-methylphenyl)-2-methyl-1,3-adamantanediamine (38).** This compound was obtained in an attempted synthesis of *rac*-**31** through the general procedure, using 1,2-dichloroethane as solvent and a reaction time of 7 h. On elution with hexane/AcOEt (90:10), adamantanediamine **38** (0.22 g, 15% yield) was isolated: mp 204−206 °C after recrystallization from hexane/AcOEt (9:1); IR 3381 (NH), 2199 (CN); ^{1}H NMR ($CDCl_3$) δ 0.94 (d, J = 7.0 Hz, 3 H, 2-CH_3), 1.65−1.70 [complex signal, 4 H, 6-H and 8(10)-H_{exo}], 1.83 [dd, J = 12.5 Hz, J' = 3.0 Hz, 2 H, 4(9)-H_{exo}], 2.03 [dm, J = 12.5 Hz, 2 H, 8(10)-H_{endo}], 2.23−2.30 (complex signal, 5-H and 7-H), superimposes in part 2.39 [dm, J = 12.5 Hz, 2 H, 4(9)-H_{endo}], 2.41 (s, 6 H, 3′-CH_3), 2.96 (q, J = 7.0 Hz, 1 H, 2-H), 4.37 (br. s, 2 H, NH), 6.54 (d, J = 7.5 Hz, 2 H, 4′-H), 6.79 (d, J = 8.5 Hz, 2 H, 6′-H), 7.19 (dd, J = 8.5 Hz, J' = 7.5 Hz, 2 H, 5′-H); ^{13}C NMR ($CDCl_3$) δ 8.7 (CH_3, 2-CH_3), 21.0 (CH_3, 3′-CH_3), 29.2 (CH) and 29.6 (CH) (C5 and C7), 35.8 (CH_2, C6), 37.3 [CH_2, C8(10)], 41.9 [CH_2, C4(9)], 43.5 (CH, C2), 56.5 [C, C1(3)], 98.7 (C, C2′), 111.0 (CH, C6′), 117.3 (C, 2′-CN), 118.0 (CH, C4′), 132.9 (CH, C5′), 143.0 (C, C3′), 148.8 (C, C1′); EI-MS m/z 410 ($M^{\bullet+}$, 9), 279 ($M^+ - C_8H_7N_2$, 100), 147 ($M^+ - 2C_8H_7N_2 - H$, 1). Anal. ($C_{27}H_{30}N_4$·1/2H_2O) C, H, N.

Biochemical Studies. AChE inhibitory activity was evaluated spectrophotometrically at 25 °C by the method of Ellman,[30] using AChE from bovine erythrocytes and acetylthiocholine iodide (0.53 mM) as substrate. The reaction took place in a final volume of 3 mL of 0.1 M phosphate-buffered solution (pH 8.0), containing 0.025 unit of AChE and 333 μM 5,5′-dithiobis(2-nitrobenzoic) acid (DTNB) solution used to produce the yellow anion of 5-thio-2-nitrobenzoic acid. Inhibition curves with different derivatives were performed in triplicate by incubating with at least 12 concentrations of inhibitor for 15 min. One triplicate sample without inhibitor was always present to yield the 100% of AChE activity. The reaction was stopped by the addition of 100 μL of 1 mM eserine, and the color production was measured at 412 nm. BChE inhibitory activity determinations were carried out similarly, using human serum BChE and butyrylthiocholine instead of AChE and acetylthiocholine.

The drug concentration producing 50% of AChE or BChE activity inhibition (IC_{50}) was calculated. Results are expressed as mean ± SEM of at least four experiments. DTNB, acetylthiocholine, butyrylthiocholine, and the enzymes were purchased from Sigma, and eserine was from Fluka.

Neuromuscular Studies. Right and left phrenic nerve-hemidiaphragms removed from male Sprague−Dawley rats (250−300 g) were used. Details of the experimental procedures have been previously described.[55] Briefly, rats were lightly anesthetized with ether and decapitated. After quick dissection, each phrenic-hemidiaphragm preparation was suspended in organ baths of 75-mL volume with Krebs-Henseleit solution of the following composition (mM): NaCl 118, KCl 4.7, $CaCl_2$ 2.5, KH_2PO_4 1.2, $NaHCO_3$ 25, and glucose 11.1. The preparation was bubbled with 5% CO_2 in oxygen, and the temperature was maintained at 25 ± 1 °C. Effects of AChE inhibitors on neuromuscular junction were assessed as the ability of reversing the partial blockade induced by *d*-tubocurarine in indirectly elicited twitch responses. The twitches were obtained by stimulating the phrenic nerve with square pulses of 0.5-ms duration at 0.2 Hz and a supramaximal voltage. Neuromuscular blockade was obtained with the addition of *d*-tubocurarine (1−1.5 μM). Drugs were added when a reduction of twitch response to 70−80% control values was obtained. The effect of each drug was evaluated after 15 min of exposure. To avoid the possible carry-over effects, only one concentration of inhibitor was tested on each preparation. Several drug concentrations were evaluated for each AChE inhibitor. To quantify the reversal effect of each drug, the antagonism index (AI or percent of antagonism)[56] was determined for each concentration and the AI_{50} (drug concentration that gives a 50% value of AI) was calculated. *d*-Tubocurarine was purchased from Sigma.

Molecular Modeling: Methods. The docking study was performed using the crystallographic structures of *T. californica* AChE liganded with THA (**1**)[19] and (−)-huperzine A (**7**).[20] The missing residues from the original PDB file[57] were built up, and their positions were refined with the AMBER program.[58] Since water molecules are essential in mediating the interaction of THA and (−)-huperzine A with AChE, all the

crystallographic water molecules were retained. The enzyme was modeled in its active form with neutral His440 and deprotonated Glu327, which form the catalytic triad together with Ser200. All other ionizable residues were considered in the standard ionization state at neutral pH, with the exceptions of Asp392 and Glu443, which were neutral, and His471, which was protonated, according to previous numerical titration calculations.[59] The resulting structure was used as the starting coordinate file in the docking study. The geometry of the inhibitors (THA, huperzine A, and hybrid derivatives) was fully optimized at the ab initio HF/6-31G(d) level using the program Gaussian 94.[60] According to the basicity for THA, huperzine A, and hybrid derivatives, the protonated species were always considered. Restricted electrostatic-potential fitted charges[61] were determined at the HF/6-31G(d) level using the standard procedure.[62,63] van der Waals parameters were taken from the values parametrized for related atom types in the AMBER force field.[58]

To examine the binding mode of the inhibitor, the structure of the inhibitor−AChE complex was energy-minimized with the AMBER program. To avoid large distortions in the enzyme, what might lead to artifactual results, the position of the water molecules was first energy-minimized for 1000 steps. Then, the enzyme−water system was reminimized for 2000 steps. Finally, the whole complex was further refined for another 2000 steps. Assuming that enzyme, inhibitors, and the enzyme−inhibitor complexes are described by their predominant conformational and ionization states, and that entropy contributions are roughly the same for the different binding modes, the differences in binding free energies were approximated as a sum of electrostatic and nonelectrostatic contributions (eq 1). The electrostatic component (ΔG_{ele}), which includes the

$$\Delta G_x = \Delta G_x(\text{ligand}-\text{AChE}) - [\Delta G_x(\text{AChE}) + \Delta G_x(\text{ligand})] \quad (1)$$

$$(x = \text{ele, n-ele})$$

solvent-screened interaction between drug and enzyme plus the electrostatic contribution due to changes in hydration, was determined from a finite difference solution of the Poisson−Boltzmann (PB) equation.[64,65] These calculations were carried out with the commonly used values of 78 and 4 for the dielectric permittivities of the aqueous and protein environments. No ionic effects were considered. To minimize the uncertainty intrinsic to the calculation, a mixed strategy combining grid rotations and the focusing method was adopted. Thus, ΔG_{ele} was averaged from the results obtained from seven independent calculations, where the grid was rotated along the different axes, and for each grid rotation, after initial solution of the PB equation, the calculation was repeated with a finer grid using the boundary conditions from the preceding calculation (the grid spacing was 1.5 and 1.1 Å). PB calculations were performed using the Delphi module implemented in Insight-II.[66] The nonelectrostatic component (ΔG_{n-ele}) was approximated from the addition of a Lennard−Jones interaction energy (ΔE_{L-J}) between drug and enzyme and a term proportional to the change in solvent-accessible surface (ΔG_{SAS}) following the linear relationship between SAS and hydrocarbon-transfer free energy observed in solubility studies of small alkanes.[67−70] Particularly, the linear dependence reported by Sitkoff et al.[69] and Tannor et al.,[70] where a single coefficient of 5 cal/(K Å^2) is assigned to the microscopic surface tension of all parts of the surface, was used.

Molecular dynamics simulations were performed using the all-atom AMBER force field for the AChE−(−)-**19** complex to verifiy the stability of the interactions between inhibitor and enzyme residues in the proposed putative binding mode. The energy-minimized structure was heated during 30 ps, and then a 500-ps molecular dynamics (T = 298 K) was performed for data collection. Indeed, we explored the effect of replacing Phe330 by Tyr, which is present in human AChE. This replacement was performed in the last structure collected from the molecular dynamics simulation. The resulting structure was energy-minimized and heated during 30 ps, and the resulting structure was used as starting point for a 500-ps molecular dynamics. The last structure was energy-minimized, and this structure was used in the computational scheme mentioned above to determine the binding free energy difference between (−)- and (+)-enantiomers of **19**.

Acknowledgment. Fellowships from Comissió Interdepartamental de Recerca i Innovació Tecnològica (CIRIT) of the Generalitat de Catalunya to J. Morral, from Agencia Española de Cooperación Internacional (Instituto de Cooperación con el Mundo Arabe, Mediterráneo y Países en Desarrollo) to R. El Achab, and from Ministerio de Educación y Cultura to X. Barril and financial support from the Comisión Interministerial de Ciencia y Tecnología (CICYT) (Programa Nacional de Tecnologías de los Procesos Químicos, Project QUI96-0828), Fundació "La Marató de TV3" (Project 3004/97), Dirección General de Investigación Científica y Técnica (Project PB97-0908), Comissionat per a Universitats i Recerca of the Generalitat de Catalunya (Project 1997-SGR-00140), and Boehringer Ingelheim España, S.A. are gratefully acknowledged. We also thank the Serveis Científico-Tècnics of the University of Barcelona and particularly Dr. A. Linares for recording the NMR spectra and Ms. P. Domènech from the Centro de Investigación y Desarrollo (C.I.D.) of Barcelona for carrying out the elemental analyses. We are indebted to Prof. Dr. A. Kozikowski (GICCS, Georgetown University, Washington, D.C.) for a generous gift of (−)-huperzine A.

Supporting Information Available: Tables of ^{13}C and ^{1}H NMR chemical shifts of **11**, **12**, and **21**−**31**. This material is available free of charge via the Internet at http://pubs.acs.org.

References

(1) Davies, P.; Malony, A. J. F. Selective Loss of Central Cholinergic Neurons in Alzheimer's Disease. *Lancet* **1976**, *2*, 1403.
(2) Perry, E. K.; Perry, R. H.; Blessed, G.; Tomlinson, B. E. Necropsy Evidence of Central Cholinergic Deficits in Senile Dementia. *Lancet* **1977**, *1*, 189.
(3) White, P.; Goodhard, M. J.; Keet, J. K.; Hiley, C. R.; Carrasio, L. H.; William, I. E. I. Neocortical Cholinergic Neurons in Elderly People. *Lancet* **1977**, *1*, 668−671.
(4) Reisine, T. D.; Yamamura, H. I.; Bird, E. D.; Spokes, E.; Enna, S. J. Pre- and Postsynaptic Neurochemical Alterations in Alzheimer's Disease. *Brain Res.* **1978**, *159*, 477−481.
(5) Davies, P. Neurotransmitter-Related Enzymes in Senile Dementia of the Alzheimer Type. *Brain Res.* **1979**, *171*, 319−327.
(6) Hollander, E.; Mohs, R. C.; Davis, K. L. Cholinergic Approaches to the Treatment of Alzheimer's Disease. *Br. Med. Bull.* **1986**, *42*, 97−100.
(7) Hershenson, F. M.; Moos, W. H. Drug Development for Senile Cognitive Decline. *J. Med. Chem.* **1986**, *29*, 1125−1130.
(8) Davis, K. L.; Powchik, P. Tacrine. *Lancet* **1995**, *345*, 625−630.
(9) Sugimoto, H.; Iimura, Y.; Yamanishi, Y.; Yamatsu, K. Synthesis and Structure−Activity Relationships of Acetylcholinesterase Inhibitors: 1-Benzyl-4-[(5,6-dimethoxy-1-oxoindan-2-yl)methyl]-piperidine Hydrochloride and Related Compounds. *J. Med. Chem.* **1995**, *38*, 4821−4829.
(10) Prous, J.; Rabasseda, X.; Castañer, J. SDZ-ENA-713 Cognition Enhancer Acetylcholinesterase Inhibitor. *Drugs Future* **1996**, *19*, 656−658.
(11) Brufani, M.; Filocamo, L.; Lappa, S.; Maggi, A. New Acetylcholinesterase Inhibitors. *Drugs Future* **1997**, *22*, 397−410.
(12) Kozikowsky, A. P.; Campiani, G.; Sun, L. Q.; Wang, S.; Saxena, A.; Doctor, B. P. Identification of a More Potent Analogue of the Naturally Ocurring Alkaloid Huperzine A. Predictive Molecular Modeling of its Interaction with AChE. *J. Am. Chem. Soc.* **1996**, *118*, 11357−11362.
(13) Harel, M.; Quin, D. M.; Nair, H. K.; Silman, I.; Sussman, J. L. The X-ray Structure of a Transition State Analogue Complex Reveals the Molecular Origins of the Catalytic Power and Substrate Specificity of Acetylcholinesterase. *J. Am. Chem. Soc.* **1996**, *118*, 2340−2346.

(14) Aguado, F.; Badia, A.; Baños, J. E.; Bosch, F.; Bozzo, C.; Camps, P.; Contreras, J.; Dierssen, M.; Escolano, C.; Görbig, D. M.; Muñoz-Torrero, D.; Pujol, M. D.; Simon, M.; Vázquez, M. T.; Vivas, N. M. Synthesis and Evaluation of Tacrine-Related Compounds for the Treatment of Alzheimer's Disease. *Eur. J. Med. Chem.* **1994**, *29*, 205−221.

(15) Pang, Y.-P.; Quiram, P.; Jelacic, T.; Hong, F.; Brimijoin, S. Highly Potent, Selective, and Low Cost Bis-Tetrahydroaminacrine Inhibitors of Acetylcholinesterase. *J. Biol. Chem.* **1996**, *271*, 23646−23649.

(16) Badia, A.; Baños, J. E.; Camps, P.; Contreras, J.; Görbig, D. M.; Muñoz-Torrero, D.; Simon, M.; Vivas, N. M. Synthesis and Evaluation of Tacrine-Huperzine A Hybrids as Acetylcholinesterase Inhibitors of Potential Interest for the Treatment of Alzheimer's Disease. *Bioorg. Med. Chem.* **1998**, *6*, 427−440.

(17) Camps, P.; Contreras, J.; Font-Bardia, M.; Morral, J.; Muñoz-Torrero, D.; Solans, X. Enantioselective Synthesis of Tacrine-Huperzine A Hybrids. Preparative Chiral MPLC Separation of their Racemic Mixtures and Absolute Configuration Assignments by X-ray Diffraction Analysis. *Tetrahedron: Asymmetry* **1998**, *9*, 835−849.

(18) Sussman, J. L.; Harel, M.; Frolow, F.; Oefner, C.; Goldman, A.; Toker, L.; Silman, I. Atomic Structure of Acetylcholinesterase from *Torpedo californica*: A Prototypic Acetylcholine-Binding Protein. *Science* **1991**, *253*, 872−879.

(19) Harel, M.; Schalk, I.; Ehret-Sabatier, L.; Bouet, F.; Goeldner, M.; Hirth, C.; Axelsen, P.; Silman, I.; Sussman, J. L. Quaternary Ligand Binding to Aromatic Residues in the Active-Site Gorge of Acetylcholinesterase. *Proc. Natl. Acad. Sci. U.S.A.* **1993**, *90*, 9031−9035.

(20) Raves, M. L.; Harel, M.; Pang, Y.-P.; Silman, I.; Kozikowski, A. P.; Sussman, J. L. Structure of Acetylcholinesterase Complexed with the Nootropic Alkaloid, (−)-Huperzine A. *Nature Struct. Biol.* **1997**, *4*, 57−63.

(21) Kimoto, K.; Imagawa, T.; Kawanisi, M. Reduction of 7-Methylenebicyclo[3.3.1]nonan-3-one and Related Compounds: Structural Investigation of the Products. *Bull. Chem. Soc. Jpn.* **1972**, *45*, 3698−3702.

(22) Liu, J.-H.; Kovacic, P. Diazotization of *endo*-7-Aminomethylbicyclo-[3.3.1]nonan-3-one and *endo*-3-Aminomethylbicyclo[3.3.1]nonane. *J. Org. Chem.* **1973**, *38*, 3462−3466.

(23) Camps, P.; El Achab, R.; Font-Bardia, M.; Görbig, D.; Morral, J.; Muñoz-Torrero, D.; Solans, X.; Simon, M. Easy Synthesis of 7-Alkylbicyclo[3.3.1]non-6-en-3-ones by Silica Gel-Promoted Fragmentation of 3-Alkyl-2-oxaadamant-1-yl Mesylates. *Tetrahedron* **1996**, *52*, 5867−5880.

(24) Schlosser, M. Organoalkali Reagents. In *Organometallics in Synthesis. A Manual*; Schlosser, M., Ed.; John Wiley & Sons: Chichester, 1994; pp 62−64.

(25) Wakefield, B. J. Organolithium Methods. In *Best Synthetic Methods*; Katritzky, A. R., Meth-Cohn, O., Rees, C. W., Eds.; Academic Press: London, 1988; pp 176−179.

(26) Imamoto, T. Organocerium Reagents. In *Comprehensive Organic Synthesis*; Trost, B. M., Fleming, I., Eds.; Pergamon Press: Oxford, 1991; Vol. 1, pp 231−250.

(27) Denmark, S. E.; Weber, T.; Piotrowski, D. W. Organocerium additions to SAMP-hydrazones: General synthesis of chiral amines. *J. Am. Chem. Soc.* **1987**, *109*, 2224−2225.

(28) Crossland, R. K.; Servis, K. L. A Facile Synthesis of Methanesulfonate Esters. *J. Org. Chem.* **1970**, *35*, 3195−3196.

(29) Kozikowski, A. P.; Campiani, G.; Tückmantel, W. An Approach to Open Chain and Modified Heterocyclic Analogues of the Acetylcholinesterase Inhibitor, Huperzine A, through a Bicyclo-[3.3.1]nonane Intermediate. *Heterocycles* **1994**, *39*, 101−116.

(30) Ellman, G. L.; Courtney, K. D.; Andres, B., Jr.; Featherstone, R. M. A New and Rapid Colorimetric Determination of Acetylcholinesterase Activity. *Biochem. Pharmacol.* **1961**, *7*, 88−95.

(31) Bowman, W. C. *Pharmacology of Neuromuscular Junction*, 2nd ed.; Butterworth: London, 1990.

(32) Kawakami, H.; Ohuchi, R.; Kitano, M.; Ono, K. Quinoline Derivatives. Patent EPO 0 268 871 A1, Sumitomo Pharmaceuticals Co., Ltd., 1987.

(33) Benzi, G.; Moretti, A. Is there a Rationale for the Use of Acetylcholinesterase Inhibitors in the Therapy of Alheimer's Disease? *Eur. J. Pharmacol.* **1998**, *346*, 1−13.

(34) Bosch, F.; Morales, M.; Badia, A.; Baños, J. E. Comparative Effects of Velnacrine, Tacrine and Physostigmine on the Twitch Responses in the Rat Phrenic-Hemidiaphragm Preparation. *Gen. Pharmacol.* **1993**, *24*, 1101−1105.

(35) Bowman, W. C.; Pryor, C.; Marshall, I. G. Presynaptic Receptors in the Neuromuscular Junction. In *Presynaptic Receptors and the Question of Autoregulation of Neurotransmitter Release;* Kalsner, S., Westfall, T. C., Eds.; New York Academy of Sciences: New York, 1990; Vol. 604, pp 69−81.

(36) Thesleff, S.; Sellin, L. C.; Tagerud, S. Tetrahydroaminoacridine (Tacrine) Stimulates Neurosecretion at Mammalian Motor Endplates. *Br. J. Pharmacol.* **1990**, *100*, 487−490.

(37) These results were estimated using the respective crystallographic structures for the enzyme complexes THA (1ACJ) and (−)-huperzine A (1VOT). However, similar values were obtained when docking of THA and (−)-huperzine A were modeled in 1VOT and 1ACJ, respectively. All subsequent calculations for the hybrid compounds were performed utilizing the enzyme structure in 1VOT.

(38) Kozikowski, A. P. Huperzine A Analogues as Acetylcholinesterase Inhibitors. U.S. Patent 5104880, 1992..

(39) Pang, Y.-P.; Hong, F.; Quiram, P.; Jelacic, T.; Brimijoin, S. Synthesis of Alkylene Linked Bis-THA and Alkylene Linked Benzyl-THA as Highly Potent and Selective Inhibitors and Molecular Probes of Acetylcholinesterase. *J. Chem. Soc., Perkin Trans. 1* **1997**, 171−176.

(40) McKinney, M.; Miller, J. H.; Yamada, F.; Tuckmantel, W.; Kozikowski, A. P. Potencies and Stereoselectivities of Enantiomers of Huperzine A for Inhibition of Rat Cortical Acetylcholinesterase. *Eur. J. Pharmacol.* **1991**, *203*, 303−305.

(41) Yamada, F.; Kozikowski, A. P.; Reddy, E. R.; Pang, Y.-P.; Miller, J. H.; McKinney, M. A Route to Optically Pure (−)-Huperzine A: Molecular Modeling and in Vitro Pharmacology. *J. Am. Chem. Soc.* **1991**, *113*, 4695−4696.

(42) Ashani, Y.; Peggins III, J. O.; Doctor, B. P. Mechanism of Inhibition of Cholinesterases by Huperzine A. *Biochem. Biophys. Res. Commun.* **1992**, *184*, 719−726.

(43) Pang, Y.-P.; Kozikowski, A. P. Prediction of the Binding of Huperzine A in Acetylcholinesterase by Docking Studies. *J. Comput.-Aided Mol. Des.* **1994**, *8*, 669−681.

(44) Ma, J. C.; Dougherty, D. A. The Cation-π Interaction. *Chem. Rev.* **1997**, *97*, 1303−1324.

(45) Cubero, E.; Luque, F. J.; Orozco, M. Is Polarization Important in Cation-π Interactions? *Proc. Natl. Acad. Sci. U.S.A.* **1998**, *95*, 5976−5980.

(46) Gregor, V. E.; Emmerling, M. R.; Lee, C.; Moore, C. J. The Synthesis and in Vitro Acetylcholinesterase and Butyrylcholinesterase Inhibitory Activity of Tacrine (Cognex) Derivatives. *Bioorg. Med. Chem. Lett.* **1992**, *2*, 861−864.

(47) Jaen, J. C.; Gregor, V. E.; Lee, C.; Davis, R.; Emmerling, M. Acetylcholinesterase Inhibition by Fused Dihydroquinazoline Compounds. *Bioorg. Med. Chem. Lett.* **1996**, *6*, 737−742.

(48) Kozikowski, A. P.; Xia, Y.; Reddy, E. R.; Tückmantel, W.; Hanin, I.; Tang, X. C. Synthesis of Huperzine A and its Analogues and their Anticholinesterase Activity. *J. Org. Chem.* **1991**, *56*, 4636−4645.

(49) Mattos, C.; Rasmussen, B.; Ding, X.; Petsko, G. A.; Ringe, D. Analogous Inhibitors of Elastase Do Not Always Bind Analogously. *Nature Struct. Biol.* **1994**, *1*, 55−58.

(50) Fisher, T. H.; Meierhoefer, A. W. Kinetic Study of the *N*-Bromosuccinimide Bromination of Some 4-Substituted 3-Cyanotoluenes. *J. Org. Chem.* **1978**, *43*, 220−224.

(51) Bogert, M. T.; Hoffman, A. Some Acyl Derivatives of Homoanthranilic Nitrile, and the 7-Methyl-4-ketodihydroquinazolines Prepared Therefrom. *J. Am. Chem. Soc.* **1905**, *27*, 1293−1301.

(52) Hunziker, F.; Fischer, R.; Kipfer, P.; Schmutz, J.; Bürki, H. R.; Eichenberger, E.; White, T. G. Seven-membered Heterocycles. 28. Neuroleptic Piperazinyl Derivatives of 10*H*-Thieno[3,2-*c*][1]-benzazepines and 4*H*-Thieno[2,3-*c*][1]benzazepines. *Eur. J. Med. Chem.* **1981**, *16*, 391−398.

(53) Preparation of isopropyllithium: Gilman, H.; Moore, F. W.; Baine, O. Secondary and Tertiary Alkyllithium Compounds and Some Interconversion Reactions with Them. *J. Am. Chem. Soc.* **1941**, *63*, 2479−2485.

(54) Preparation of allyllithium: Wakefield, B. J. Organolithium Methods. In *Best Synthetic Methods*; Katritzky, A. R., Meth-Cohn, O., Rees, C. W., Eds.; Academic Press: London, 1988; pp 47−49.

(55) Baños, J. E.; Badia, A.; Jané, F. Facilitatory Action of Adrenergic Drugs on Muscle Twitch Evoked by Nerve Stimulation in the Curarized Rat Phrenic-Hemidiaphragm. *Arch. Int. Pharmacodyn.* **1988**, *293*, 219−227.

(56) Riesz, M.; Kapati, E.; Szporni, L. Antagonism of Non-Depolarizing Neuromuscular Blockade by Aminopyridines in Cats. *J. Pharm. Pharmacol.* **1986**, *38*, 156−158.

(57) Protein Data Bank entries are 1ACJ (tacrine−AChE−tacrine) and 1VOT [(−)-huperzine A-AChE].

(58) Pearlman, D. A.; Case, D. A.; Caldwell, J. C.; Ross, W. S.; Cheatham, T. E.; Ferguson, D. M.; Seibel, G. L.; Singh, U. C.; Weiner, P.; Kollman, P. A. *AMBER 4.1*; University of California: San Francisco, 1995.

(59) Wlodek, S. T.; Antosiewicz, J.; McCammon, J. A.; Straatsma, T. P.; Gilson, M. K.; Briggs, J. M.; Humblet, C.; Sussman, J. L. Binding of Tacrine and 6-Chlorotacrine by Acetylcholinesterase. *Biopolymers* **1996**, *38*, 109−117.

(60) Frisch, M. J.; Trucks, G. W.; Schlegel, H. B.; Gill, P. M. W.; Johnson, B. G.; Robb, M. A.; Cheeseman, J. R.; Keith, T. A.; Petersson, G. A.; Montgomery, J. A.; Raghavachari, K.; Al-Laham, M. A.; Zakrzewski, V. G.; Ortiz, J. V.; Foresman, J. B.; Cioslowski, J.; Stefanov, B. B.; Nanayakkara, A.; Challacombe,

M.; Peng, C. Y.; Ayala, P. Y.; Chen, W.; Wong, M. W.; Andres, J. L.; Replogle, E. S.; Gomperts, R.; Martin, R. L.; Fox, D. J.; Binkley, J. S.; Defrees, D. J.; Baker, J.; Stewart, J. P.; Head-Gordon, M.; Gonzalez, C.; Pople, J. A. *Gaussian 94*, Rev. A.1; Gaussian Inc.: Pittsburgh, 1995.

(61) Cornell, W. D.; Cieplak, P.; Baily, C. I.; Kollman, P. A. Application of RESP Charges to Calculate Conformational Energies, Hydrogen Bond Energies, and Free Energies of Solvation. *J. Am. Chem. Soc.* **1993**, *115*, 9620−9631.

(62) Singh, U. C.; Kollman, P. A. An Approach to Computing Electrostatic Charges for Molecules. *J. Comput. Chem.* **1984**, *5*, 129−145.

(63) Orozco, M.; Luque, F. J. On the Use of AM1 and MNDO Wave functions to Compute Accurate Electrostatic Charges. *J. Comput. Chem.* **1990**, *8*, 909−923.

(64) Gilson, M. K.; Honig, B. H. Calculation of the Total Electrostatic Energy of a Macromolecular System: Solvation Energies, Binding Energies, and Conformational Analysis. *Proteins* **1988**, *4*, 7−18.

(65) Gilson, M. K.; Sharp, K. A.; Honig, B. H. Calculating the Electrostatic Potential of Molecules in Solution: Method and Error Assessment. *J. Comput. Chem.* **1988**, *9*, 327−335.

(66) *Insight-II*; Biosym Technologies: San Diego, 1993.

(67) Eisenberg, D.; McLachlan, A. D. Solvation Energy in Protein Folding and Binding. *Nature* **1986**, *319*, 199−203.

(68) Hermann, R. B. Modeling Hydrophobic Solvation of Nonspherical Systems: Comparison of Use of Molecular Surface Area with Accessible Surface Area. *J. Comput. Chem.* **1997**, *18*, 115−125.

(69) Sitkoff, D.; Sharp, K. A.; Honig, B. Accurate Calculation of Hydration Free Energies Using Macroscopic Solvent Models. *J. Phys. Chem.* **1994**, *98*, 1978−1988.

(70) Tannor, D. J.; Marten, B.; Murphy, R.; Friesner, R. A.; Sitkoff, D.; Nicholls, A.; Ringnalda, M.; Goddard, W. A., III; Honig, B. Accurate First Principles Calculation of Molecular Charge Distributions and Solvation Energies from ab initio Quantum Mechanics and Continuum Dielectric Theory. *J. Am. Chem. Soc.* **1994**, *116*, 11875−11882.

JM980620Z